Biotechnology Research and Innovation, 2025, 9(2): e2025007. https://doi.org/10.4322/biori.00072025

Biotechnology Research & Innovation

www.biori.periodikos.com.br

RESEARCH PAPERS

In silico screening of multi-target drugs against Alzheimer's Disease: a repurposing approach

Mariana Bertoldi Amato[a,#], Daniela Peres Martinez[a], Rafaella Sinnott Dias[a], Fabiane Neitzke Höfs[a,#], Frederico Schmitt Kremer[a,*]

[a]*Center for Technological Development, Federal University of Pelotas - UFPel, UFPel Campus, CEP 96160-000, Capão do Leão, RS, Brazil*
[#]These authors contributed equally to the execution of the present work.

Highlights

- FDA drugs screened with validated QSAR models for multi-target AD activity
- Applicability domain analysis supported the reliability of the predictions
- Antipsychotics showed high affinity for AChE, BACE1, and MAO-B
- Droperidol and Pimozide were identified as multi-target candidates
- Ibutilide was identified as a novel dual-target candidate

Received 23 July, 2025; Accepted 03 January, 2026.

KEYWORDS
Chemoinformatics; Drug discovery; Structural bioinformatics; Neurodegenerative diseases; Dementia.

Abstract: Alzheimer's Disease (AD) is characterized by complex pathophysiology involving beta-amyloid plaques and neurofibrillary tangles, for which current therapies have limited efficacy. To address the multifactorial nature of AD, this study investigated the hypothesis that existing FDA-approved drugs can be repurposed as multi-target agents by computationally screening for simultaneous activity against key pathological drivers. We developed a pipeline of predictive Quantitative Structure-Activity Relationship (QSAR) models for critical AD-related targets, including AChE, BACE1, and proteins involved in tau pathology. The methodological rigor of these models, which primarily leveraged the Extremely Randomized Tree algorithm, was ensured through robust validation techniques including cross-validation, y-randomization, and a thorough applicability domain analysis. Our virtual screening identified several FDA-approved drugs, notably antipsychotics like Droperidol and Pimozide, as high-potential multi-target candidates. Subsequent molecular docking analysis revealed plausible binding modes for these candidates within the active sites of key targets. While these computational results suggest promising mechanisms for inhibiting multiple disease pathways, they require definitive experimental validation to confirm their effectiveness. By shifting the focus from automation to insight, this work provides a validated computational framework that generates testable hypotheses for drug repurposing in AD and prioritizes specific, clinically-approved molecules for future investigation into their potential multi-target efficacy.

*Corresponding author.
E-mail: fred.s.kremer@gmail.com (F. S. Kremer).

Graphical Abstract

In Silico Multi-Target Drug Discovery Pipeline using QSAR and Molecular Docking

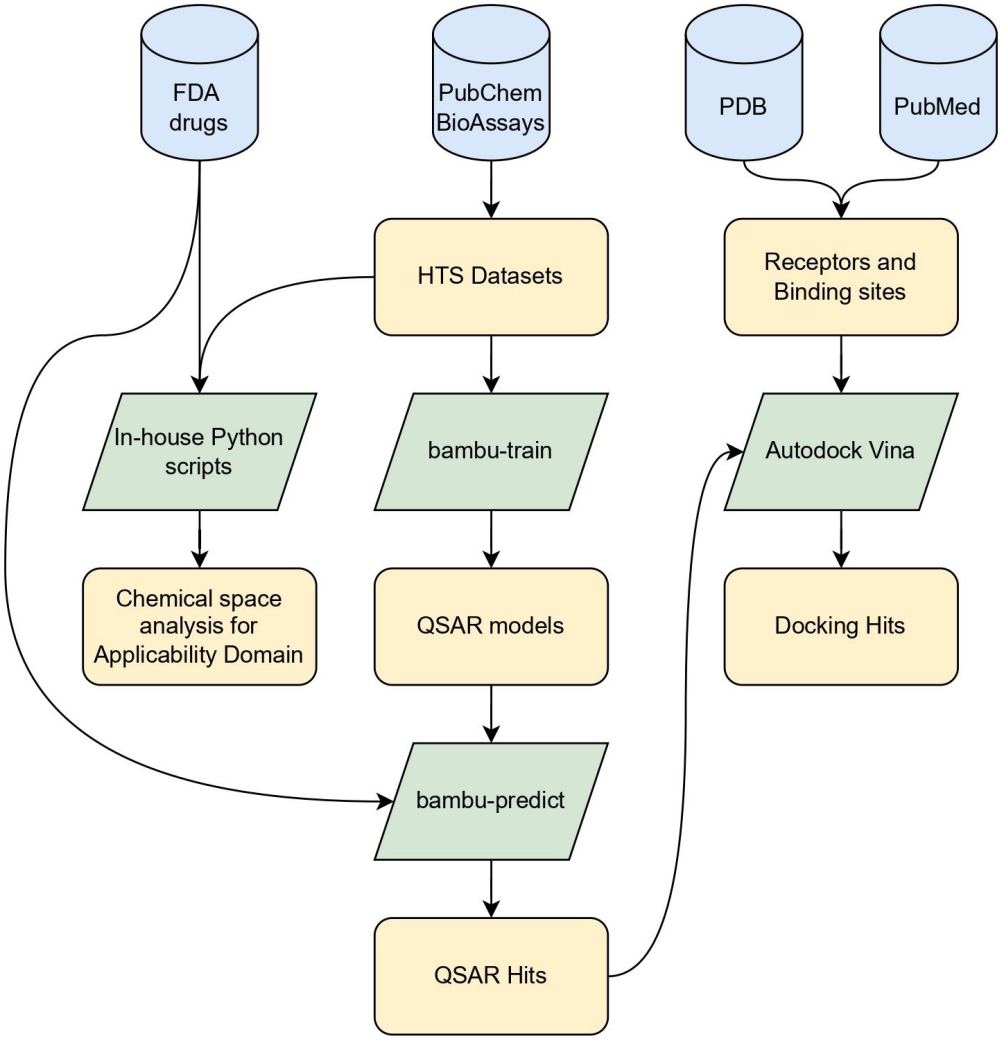

Introduction

Alzheimer's disease (AD) is characterized by degenerative processes affecting cognition, behavior, and function, typically beginning with a decline in memory of recent events (Scheltens et al., 2016; Zhang et al., 2021). It is a neurodegenerative disease that occurs progressively, starting in the asymptomatic preclinical form, progressing to mild cognitive impairment, and evolving in mild, moderate, and severe degrees (Swanson et al., 2021). The main risk factor linked to the development of the disease is aging, added to the increase in life expectancy of the population, AD is currently identified as the primary and most prevalent form of dementia (Breijyeh & Karaman, 2020; Kumar et al., 2022).

Among the brain changes linked to AD are the accumulation of fragments of the ß-amyloid protein (outside of neurons) and an atypical accumulation of the hyperphosphorylated forms of the tau protein (inside of neurons). These changes lead to cell death and eventual neurodegeneration, primarily affecting regions such as the hippocampus and cortex, which are involved in learning, perception, and memory (DeTure & Dickson, 2019). These characteristics of the disease are essential because the pathogenesis of AD can begin with the formation of ß-amyloid oligomers, which are capable of triggering a succession of events, including oxidative stress and tau neurofibrillary tangles (Miller et al., 2022). In this context, significant brain changes, including inflammation and atrophy, occur in individuals affected by the disease.

Chronic inflammation occurs when microglia are unable to efficiently eliminate toxic ß-amyloid and tau proteins; atrophy, on the other hand, results from cell loss that is a natural part of the disease's progression. In addition to the factors mentioned, there is a decrease in the ability to metabolize glucose (DeTure & Dickson, 2019).

Regarding drug therapy, the available medications aim to mitigate the individual's cognitive and behavioral deficits, rather than interrupting or delaying the pathophysiological progression of the disease. In this perspective, only a few drugs have been approved for the treatment of AD, of which three act by inhibiting the enzyme acetylcholinesterase (AChE): rivastigmine, galantamine, and donepezil. It should be noted that this class of drugs is recommended in the initial phase and has a series of side effects, mainly gastrointestinal (Marucci et al., 2021). It is noteworthy that tacrine, previously included in this group, had its use discontinued due to its liver toxicity (Breijyeh & Karaman, 2020). Another drug used is memantine, a non-competitive antagonist of the glutamate receptor (NMDA), indicated for the treatment of moderate to severe stages of the disease (Tang et al., 2023). However, the therapeutic strategies currently employed are ineffective in combating the disease due to the pathophysiological complexity involved in the disease process, which is still poorly understood, posing a significant challenge for neuroscience (Kumar et al., 2022).

The development of multi-target drugs, molecules able to interact selectively with different molecular targets, is a promising approach for developing new treatments against AD. Additionally, the application of computational methods, such as QSAR and molecular docking, enables the virtual screening of molecule libraries and accelerates the identification of new candidates for further *in vitro* and *in vivo* testing in drug discovery pipelines. Finally, the repurposing of molecules already approved for human use by regulatory agencies (eg, FDA) might accelerate the availability of new treatments for AD. Therefore, here we describe a virtual screening for multi-target repurposed drugs against AD, using a combination of QSAR, molecular docking, and a dataset from FDA-approved drugs.

Material and methods

QSAR modelling

QSAR models were trained using HTS data available in PubChem BioAssays for various AD molecular targets. Furthermore, a model for Blood-Brain Barrier (BBB) permeability was trained using the B3DB dataset. Selected datasets are displayed in Table 1. All QSAR models were trained using the BAMBU package (Guidotti et al., 2023), which automates the downloading, preprocessing, training, and validation of QSAR models. However, while BAMBU automates several routine data processing and training tasks, it is crucial to note that the entire workflow was implemented as a manually configured script. All parameters for data preprocessing, feature selection, algorithm choice, and validation were explicitly defined to ensure complete transparency, control, and scientific reproducibility. This scripted approach avoids a "black-box" scenario, allowing for a customized and rigorously controlled pipeline explicitly tailored to the hypotheses of this investigation.

As features, we evaluated the use of molecular descriptors, Morgan Fingerprints (1024 and 2048 bits), and Mol2Vec representations. Molecular descriptors and fingerprint calculations are performed using RDKit, while Mol2Vec representations are generated based on the implementations available at GitHub (2023). For model selection, BAMBU relies on FLAML (2023) for automated machine learning (AutoML), enabling the selection and hyperparameter optimization of various algorithms, including Logistic Regression (LR), Random Forest (RF), Extremely Randomized Trees (ERT), and Gradient Boosting Trees (GB).

All datasets were balanced using random under-sampling and randomly split into train and test datasets after duplicate removal (75% training, 25% test). Models were selected based on the F1-score metric, and also evaluated using the accuracy, precision, recall, and F1-score.

Evaluation of applicability domain

To evaluate the Applicability Domain, two approaches were used: Convex Hull (CH) and Kernel-Based Estimation. Both methods were applied based on 2D embeddings generated using UMAP from the feature space produced by the preprocessing step. The Convex Hull was generated using SciPy based on the embeddings from the training dataset, and molecules from the FDA dataset outside the CH were identified. For the Kernel-Based method, the UMAP embeddings from the training dataset were used to fit a KernelDensity estimator from Scikit-Learn, which was used to compute the log-likelihood distribution of each molecule from the training and FDA datasets. Then, the log-likelihoods from each molecule in the FDA dataset were compared to those from the training dataset using the Kolmogorov-Smirnov test from SciPy. The p-values were then adjusted using the statsmodels package's FDR correction method, and molecules with a corrected p-value < 0.05 were identified as being outside the Applicability Domain.

QSAR virtual screening

Based on the trained models, a ligand-based screening of FDA-approved drugs for human use was performed aiming to identify ligands able to inhibit APP (probability > 50%), inhibit tau (probability > 50%), bind to tau (probability > 50%) and inhibit AChE (probability > 50%), do not inhibit CHRM1, CHRM4 and CHRM5 (probability < 5%), do not activate tau (probability < 5%) while being able to pass the blood-brain barrier (probability > 50%) and not activate NF-kB (probability < 5%).

Molecular docking and protein-ligand interaction fingerprint analysis

Protein-ligand molecular docking simulations were performed using AutoDock Vina (Trott & Olson, 2010), with ligand and receptor structures prepared using AutoDockTools (Morris et al., 2009). The structures of the target proteins

Table 1. HTS datasets were obtained from PubChem BioAssays for different types of anti-Alzheimer's targets.

BioAssays ID	Target	Effect	Molecules		Criteria for Activity
			Active	Inactive	(based on PubChem BioAssays available metadata)
1239	NF-kB	agonist	3,100	190,164	Compounds were classified as "Active" if they demonstrated a fold increase in luminescence greater than or equal to 3.3 compared to the median cell control.
1276	Amyloid Precursor Peptide	activator	1,987	191,413	A compound was classified as "Active" if it resulted in a percent activation greater than 135%, a threshold defined as the average of control wells plus three standard deviations.
1285	Amyloid Precursor Peptide	inhibitor of expression	1,590	192,124	A compound was classified as "Active" if it exhibited a percent inhibition greater than 45%, a threshold calculated as the average of the controls plus three standard deviations.
1468	Tau Protein	Inhibitor of aggregation	1,048	251,327	A compound was classified as "Active" if it produces a measurable dose-response curve, which is then qualitatively classified by its shape (e.g., 'full curve', 'partial curve', or 'single-point activity').
588852	CHRM1	antagonist	4,555	354,661	A compound was classified as "Active" if its percent inhibition was greater than a plate-specific cutoff, which was calculated as the sum of the average percent inhibition of all test compounds on that plate plus three times their standard deviation.
602250	CHRM1	antagonist	2,168	359,861	A compound was classified as "Active" if its percent inhibition was greater than a plate-specific cutoff, which was calculated as the sum of the average percent inhibition of all test compounds on that plate plus three times their standard deviation.
624040	CHRM5	antagonist	2,133	361,677	A compound was classified as "Active" if its percent inhibition was greater than a plate-specific cutoff, which was calculated as the sum of the average percent inhibition of all test compounds on that plate plus three times their standard deviation.
624125	CHRM4	antagonist	2,629	361,186	A compound was classified as "Active" if its percent inhibition was greater than a plate-specific cutoff, which was calculated as the sum of the average percent inhibition of all test compounds on that plate plus three times their standard deviation.
1347395	AChE	inhibitor	388	7,021	A compound was classified as "Active" if it produces a measurable dose-response curve, which is then qualitatively classified by its shape (e.g., 'full curve', 'partial curve', or 'single-point activity').
1347398	AChE	inhibitor	336	6,870	A compound was classified as "Active" if it produces a measurable dose-response curve, which is then qualitatively classified by its shape (e.g., 'full curve', 'partial curve', or 'single-point activity').
B3DB*	N/A	BBB permeability	4,956	2,851	A compound is defined as BBB+ (Active) or BBB− (Inactive) using a logBB value of -1 as the threshold, considering data extracted from literature and other sources.

*Derived from the B3DB dataset.

(receptors) were obtained from the PDB, and residues related to biological activity were extracted from previous works describing mechanisms of action and molecular docking studies, as presented in Table 2. For each target structure, a grid box was created around the selected residues with a padding of 10 Ängstrons in the three axes. Docking results were processed using PLIP (Adasme et al., 2021; Salentin et al., 2015), and binding interactions were used to compute a score for each protein-ligand complex based on the percentage of "relevant" residues (derived from literature) with predicted interactions for a particular ligand. These Protein-Ligand Interaction Fingerprints (PLIFs) were used to compute an average score based on all targets used, and it was used to rank the molecules in the FDA dataset. The high-affinity targets were defined as those whose binding energy was <= 7.0 kcal/mol, with a 0.3 kcal/mol penalty per heavy atom in the ligand (Ivanova & Karelson, 2022; Zhu et al., 2013). Only molecules with at least one high-affinity target were selected. The top 20 molecules were selected for further analysis.

ADMET and PAINS

Pharmacokinetic and Toxicological properties of the selected molecules were computed using ADMETLab (Xiong et al., 2021), while structural alerts for molecular promiscuity were analyzed using PAINS Remover (Baell & Holloway, 2010). Finally, molecules with undesirable properties in any of these tools were excluded from the final list.

Results

Ligand-based and receptor-based virtual screening results

Results of the model training and selection are presented in Supplementary Data 2, and the best models for each bioassay dataset are summarized in Table 2. A key finding was that almost all selected models are based on the Extremely Randomized Tree algorithm (extra_tree), an ensemble of decision-tree classifiers, suggesting this algorithm's effectiveness for the diverse datasets and targets investigated. The models primarily utilized Morgan fingerprints of size 1024 or 2048 bits as molecular descriptors, indicating the importance of substructure features in predicting activity against the Alzheimer's Disease targets. The F1-scores for the models ranged from 57.12 to 88.08, demonstrating varying levels of predictive performance across the different bioassays. Accuracy scores ranged from 57.47 to 87.8%, further illustrating the models' ability to classify active and inactive compounds.

The results from the analysis of the Applicability Domain are presented in Supplementary Data 3 and summarized in Table 3.

Table 2. The best model was selected for each molecular target and their respective classification metrics after model evaluation using the test dataset. All metrics were calculated using balanced test datasets to ensure robust evaluation.

BioAssays ID	descriptors	algorithm	Default					Y-Randomization				
			Accuracy	Recall	Precision	F1	ROC-AUC	Accuracy	Recall	Precision	F1	ROC-AUC
1239	morgan-1024	ET	0.81	0.81	0.82	0.82	0.89	50.32 ∓ 0.02	48.36 ∓ 0.02	52.09 ∓ 0.02	50.15 ∓ 0.02	50.28 ∓ 0.02
1276	morgan-1024	ET	0.84	0.83	0.86	0.84	0.92	50.13 ∓ 0.02	48.63 ∓ 0.02	51.40 ∓ 0.02	49.96 ∓ 0.02	49.78 ∓ 0.02
1285	morgan-2048	ET	0.75	0.70	0.79	0.74	0.83	49.81 ∓ 0.02	49.59 ∓ 0.03	50.26 ∓ 0.02	49.90 ∓ 0.02	49.83 ∓ 0.02
1468	morgan-1024	ET	0.86	0.85	0.86	0.85	0.93	50.07 ∓ 0.03	51.45 ∓ 0.03	48.61 ∓ 0.03	49.97 ∓ 0.03	50.19 ∓ 0.04
588852	morgan-2048	ET	0.76	0.70	0.80	0.75	0.84	50.22 ∓ 0.01	49.57 ∓ 0.02	50.75 ∓ 0.01	50.15 ∓ 0.01	50.08 ∓ 0.01
602250	morgan-2048	ET	0.60	0.54	0.63	0.58	0.63	50.04 ∓ 0.02	48.29 ∓ 0.02	52.25 ∓ 0.02	50.18 ∓ 0.02	50.03 ∓ 0.02
624040	morgan-2048	ET	0.75	0.69	0.78	0.73	0.82	49.84 ∓ 0.02	50.52 ∓ 0.03	49.34 ∓ 0.02	49.91 ∓ 0.02	50.05 ∓ 0.03
624125	descriptors	ET	0.76	0.68	0.79	0.73	0.83	49.85 ∓ 0.02	52.21 ∓ 0.02	48.38 ∓ 0.02	50.21 ∓ 0.02	50.20 ∓ 0.02
1347395	mol2vec	ET	0.80	0.82	0.79	0.81	0.86	50.95 ∓ 0.05	51.59 ∓ 0.07	50.43 ∓ 0.05	50.92 ∓ 0.05	50.88 ∓ 0.07
1347398	descriptors	RF	0.79	0.75	0.82	0.79	0.86	50.30 ∓ 0.05	49.46 ∓ 0.07	50.95 ∓ 0.05	50.07 ∓ 0.05	50.42 ∓ 0.06
B3DB*	morgan-1024	ET	0.98	0.96	0.99	0.97	1.00	55.02 ∓ 0.01	35.13 ∓ 0.01	45.27 ∓ 0.01	39.56 ∓ 0.01	49.26 ∓ 0.01

*Derived from the B3DB dataset.

Table 3. Analysis of the Applicability Domain of the QSAR models trained from different BioAssays for Alzheimer's Disease targets derived from PubChem and Blood-Brain Barrier Permeability (B3DB), including the number of molecules outside the Applicability Domain estimated using two methods: Convex Hull and Kernel Density.

BioAssay ID	Convex Hull		Kernel Density	
	Count	Percent	Count	Percent
1239	3	0.19%	0	0.00%
1276	0	0.00%	0	0.00%
1285	2	0.12%	0	0.00%
1468	54	3.34%	0	0.00%
588852	1	0.06%	0	0.00%
602250	3	0.19%	0	0.00%
624040	4	0.25%	0	0.00%
624125	0	0.00%	0	0.00%
1347395	76	4.71%	0	0.00%
1347398	57	3.53%	0	0.00%
B3DB	2	0.12%	0	0.00%

The distribution of the FDA molecules largely fell within the training dataset distribution, which is crucial for ensuring the reliability of the model predictions. When considering the Convex Hull method, a few exceptions were observed, indicating some FDA molecules were at the edge of the training data's chemical space. However, no molecule outside the distribution was identified when considering the Kernel Density method, a more nuanced approach that estimates the probability density of the training data. This suggests that the FDA dataset is generally within the Applicability Domain of the QSAR models, validating the use of these models for virtual screening.

Using the model predictions for the FDA dataset, molecules with a Blood-Brain Barrier (BBB) permeability probability estimated to be equal to or greater than 75% were selected, ensuring that the identified compounds have the potential to reach the brain. These molecules were ranked based on an average prediction score, resulting in 427 molecule candidates, which are presented in Supplementary Data 4 and were selected for the docking step. Importantly, none of these molecules presented PAINS patterns or pharmacokinetics issues based on the ADMETLab and PAINS Remover reports, respectively, ensuring that the selected compounds have a favorable profile for further development. Finally, binding energies from the molecular docking analysis are presented in Supplementary Data 5, including residues of protein-ligand interactions and binding energies, while significant hits are summarized in Table 4.

Table 4. Top 20 molecules from the FDA with high-affinity targets identified by molecular docking for multiple targets of Alzheimer's Disease. Binding energy (BE) and Ligand Efficiency (LE) are displayed in kcal / mol. Protein-Ligand Interaction Fingerprint (PLIF) was compared to residues previously described in the literature as relevant for the activity of molecules targeting the protein, and a Tanimoto (Jaccard) similarity was computed.

ZINC ID	DrugBank ID	Drug Name	Target PDB	Target Name	BE	LE	Interactions	PLIF Tanimoto
ZINC000082144002	DB00308	Ibutilide	1ACJ	AChE	-8.12	-0.31	Trp279 (A), Tyr130 (A), Trp84 (A), Asp72 (A), Phe330 (A), Tyr70 (A), Tyr334 (A)	40.0%
			4A79	MAO-B	-8.71	-0.34	Trp119 (A), Ile316 (A), Phe103 (A), Tyr326 (A), Gln206 (A), Phe343 (A), Phe168 (A), Tyr398 (A), Leu171 (A)	4.55%
			1GOS	MAO-B	-8.51	-0.33	Met436 (A), Gln206 (A), Phe343 (A), Tyr60 (A), Tyr398 (A), Tyr435 (A)	17.65%
ZINC000019796080	DB00450	Droperidol	4PQE	AChE	-10.38	-0.37	Trp286 (A), Asp74 (A), Tyr341 (A), His447 (A), Tyr337 (A), Trp86 (A)	50.0%
			4BDT	AChE	-10.83	-0.39	Thr83 (A), Asp74 (A), Gly120 (A), Tyr341 (A), Tyr133 (A), Trp439 (A), Tyr337 (A), Trp86 (A)	62.5%
			1ACJ	AChE	-11.38	-0.41	Trp279 (A), Tyr442 (A), Tyr121 (A), Trp84 (A), Asp72 (A), Phe330 (A), Tyr70 (A), Tyr334 (A)	60.0%
			2QP8	BACE1	-8.7	-0.31	Asp93 (A), Ile171 (A), Gln134 (A), Tyr132 (A), Leu91 (A), Trp176 (A), Thr133 (A), Phe169 (A)	50.0%
			5HU1	BACE1	-8.67	-0.31	Gly95 (A), Tyr132 (A), Leu91 (A), Trp176 (A), Tyr259 (A), Ile179 (A)	28.57%
			5I3V	BACE1	-9.38	-0.33	Phe108 (A), Leu30 (A), Asp32 (A), Asn37 (A), Ile118 (A), Tyr14 (A), Trp76 (A), Val69 (A)	36.36%
			4DJU	BACE1	-8.58	-0.31	Tyr132 (A), Val130 (A), Arg189 (A), Phe169 (A), Asn98 (A), Tyr259 (A)	50.0%
			1P0P	BuChE	-9.89	-0.35	Trp82 (A), Phe329 (A), Ser198 (A), Ala328 (A), Gly117 (A), Gly116 (A), Tyr332 (A)	50.0%
			3POZ	EGFR	-9.25	-0.33	Leu844 (A), Phe856 (A), Phe997 (A), Lys745 (A), Met766 (A), Ala743 (A), Leu718 (A), Val726 (A)	22.22%
			1UV5	GSK-3β	-9.53	-0.34	Val70 (A), Leu132 (A), Leu188 (A), Asp200 (A), Val110 (A), Val135 (A), Ile62 (A)	25.0%
			4A79	MAO-B	-11.26	-0.4	Ala35 (A), Tyr393 (A), Leu268 (A), Thr43 (A), Ala439 (A), Val235 (A), Arg42 (A), Ile14 (A), Arg36 (A), Lys271 (A), Glu34 (A)	31.82%
			1GOS	MAO-B	-11.27	-0.4	Ala35 (A), Ala439 (A), Leu268 (A), Ile264 (A), Tyr393 (A), Thr426 (A), Ile14 (A), Ser15 (A), Glu34 (A), Lys271 (A), Gly12 (A)	29.41%
			1PME	MAPK1	-8.51	-0.3	Lys54 (A), Leu75 (A), Val39 (A), Ala52 (A), Thr105 (A), Ile84 (A), Lys114 (A), Asp167 (A), Leu156 (A), Leu103 (A), Met108 (A)	100.0%
			5K4I	MAPK1	-9.36	-0.33	Ile56 (A), Gln105 (A), Lys54 (A), Ile31 (A), Val39 (A), Asp167 (A), Leu156 (A), Tyr36 (A)	55.56%
			5ES1	MARK4	-9.31	-0.33	Val70 (A), Tyr134 (A), Ala83 (A), Glu139 (A), Lys85 (A), Ala195 (A), Glu182 (A), Ile62 (A), Val116 (A)	71.43%

Table 4. Continued...

ZINC ID	DrugBank ID	Drug Name	Target PDB	Target Name	BE	LE	Interactions	PLIF Tanimoto
ZINC000004175630	DB01100	Pimozide	1ACJ	AChE	-11.24	-0.33	Trp279 (A), His440 (A), Phe290 (A), Trp84 (A), Phe331 (A), Asp72 (A), Phe330 (A), Tyr70 (A), Tyr334 (A)	40.0%
			5I3V	BACE1	-10.37	-0.3	Phe108 (A), Ile110 (A), Leu30 (A), Asp106 (A), Asp32 (A), Tyr71 (A), Asn37 (A), Trp76 (A), Val69 (A), Lys107 (A), Trp115 (A)	54.55%
			1P0P	BuChE	-11.01	-0.32	Trp82 (A), Phe329 (A), Ala328 (A), His438 (A), Asp70 (A), Thr120 (A), Leu125 (A), Tyr332 (A), Leu286 (A)	100.0%
			4A79	MAO-B	-12.48	-0.37	Lys296 (A), Thr43 (A), Arg42 (A), Thr426 (A), Ile14 (A), Ser15 (A), Phe343 (A), Tyr398 (A), Tyr435 (A)	31.82%
			1GOS	MAO-B	-12.33	-0.36	Ala439 (A), Tyr326 (A), Arg42 (A), Ile14 (A), Gln206 (A), Gly434 (A), Phe343 (A), Tyr60 (A), Tyr398 (A), Leu171 (A), Tyr435 (A)	41.18%
			5K4I	MAPK1	-10.63	-0.31	Lys54 (A), Ile31 (A), Val39 (A), Ala52 (A), Asp167 (A), Leu156 (A), Met108 (A)	77.78%
ZINC000001886617	DB01095	Fluvastatin	4BDT	AChE	-10.3	-0.34	Ser125 (A), Tyr133 (A), His447 (A), Tyr449 (A), Trp439 (A), Pro446 (A), Tyr337 (A), Trp86 (A)	37.5%
			1ACJ	AChE	-9.37	-0.31	Trp279 (A), Ile439 (A), Trp432 (A), Tyr442 (A), Tyr121 (A), Trp84 (A), Phe330 (A), Tyr70 (A), Tyr334 (A)	60.0%
			1P0P	BuChE	-9.54	-0.32	Trp82 (A), Phe329 (A), Ser198 (A), Ala328 (A), Gly117 (A), Tyr440 (A), Trp430 (A), Tyr332 (A), Leu286 (A)	50.0%
			1UV5	GSK-3β	-9.12	-0.3	Asn64 (A), Tyr134 (A), Leu132 (A), Leu188 (A), Ala83 (A), Asp200 (A), Lys85 (A), Val110 (A), Ile62 (A), Thr138 (A), Phe67 (A), Ser66 (A)	41.67%
			1GOS	MAO-B	-9.19	-0.31	Lys296 (A), Arg42 (A), Gln206 (A), Phe343 (A), Tyr398 (A), Tyr435 (A)	11.76%
ZINC000001535101	DB01098	Rosuvastatin	1ACJ	AChE	-9.91	-0.3	Gly119 (A), Ile439 (A), His440 (A), Trp432 (A), Glu199 (A), Tyr442 (A), Ser122 (A), Tyr121 (A), Trp84 (A), Asp72 (A), Phe330 (A), Ser200 (A)	20.0%
ZINC000001996117	DB00496	Darifenacin	4PQE	AChE	-11.35	-0.35	Tyr124 (A), Phe338 (A), Asp74 (A), Glu202 (A), Ser203 (A), Trp439 (A), Gly121 (A), Tyr337 (A), Trp86 (A), Phe297 (A)	50.0%
			4BDT	AChE	-12.05	-0.38	Tyr124 (A), Asp74 (A), Gly120 (A), Ser203 (A), Leu130 (A), Glu202 (A), Tyr337 (A), Trp86 (A), Phe297 (A)	37.5%
			1ACJ	AChE	-10.83	-0.34	Glu199 (A), Tyr121 (A), Phe331 (A), Trp84 (A), Phe330 (A), Ser200 (A)	20.0%
			5HU1	BACE1	-10.1	-0.32	Ile171 (A), Gln134 (A), Tyr132 (A), Thr293 (A), Phe169 (A), Ile179 (A)	42.86%
			2WJO	BACE1	-9.7	-0.3	Phe108 (A), Gly34 (A), Ile110 (A), Leu30 (A), Thr232 (A), Asp32 (A), Tyr71 (A), Asn37 (A), Ile118 (A), Trp76 (A), Val69 (A), Trp115 (A)	50.0%
			1P0P	BuChE	-10.71	-0.33	Trp82 (A), Phe329 (A), Ser198 (A), Ala328 (A), Tyr332 (A), Glu197 (A)	50.0%
			3POZ	EGFR	-10.15	-0.32	Leu844 (A), Arg841 (A), Phe997 (A), Lys745 (A), Ala743 (A), Leu718 (A), Met793 (A), Val726 (A), Leu1001 (A), Phe723 (A)	22.22%
			4A79	MAO-B	-11.3	-0.35	Lys296 (A), Ser59 (A), Thr426 (A), Ile14 (A), Ser15 (A), Phe343 (A), Tyr60 (A), Tyr398 (A), Tyr435 (A)	31.82%
			1GOS	MAO-B	-11.32	-0.35	Ala439 (A), Ser59 (A), Arg42 (A), Thr426 (A), Ile14 (A), Phe343 (A), Tyr60 (A), Tyr398 (A), Tyr435 (A)	35.29%

Table 4. Continued...

ZINC ID	DrugBank ID	Drug Name	Target PDB	Target Name	BE	LE	Interactions	PLIF Tanimoto
ZINC000004095858	DB00163	alpha-tocopherol (Vitamin E)	4PQE	AChE	-9.41	-0.3	Phe338 (A), Trp286 (A), Asp74 (A), Tyr341 (A), Tyr72 (A), Tyr337 (A), Trp86 (A), Phe297 (A)	25.0%
			4BDT	AChE	-9.48	-0.31	Phe338 (A), Phe295 (A), Tyr341 (A), Tyr449 (A), Trp439 (A), Pro31 (B), Tyr337 (A), Trp86 (A), Phe297 (A)	50.0%
			1ACJ	AChE	-10.71	-0.35	Trp279 (A), Ile287 (A), His440 (A), Trp432 (A), Phe290 (A), Tyr442 (A), Trp84 (A), Phe331 (A), Asp72 (A), Phe330 (A), Tyr70 (A), Tyr334 (A)	40.0%
			4A79	MAO-B	-10.26	-0.33	Trp119 (A), Ile316 (A), Tyr326 (A), Ile199 (A), Leu164 (A), Phe343 (A), Tyr60 (A), Pro104 (A), Tyr398 (A), Leu171 (A), Tyr435 (A), Phe168 (A)	13.64%
			1GOS	MAO-B	-10.57	-0.34	Trp119 (A), Phe103 (A), Leu167 (A), Tyr326 (A), Ile199 (A), Leu164 (A), Phe343 (A), Tyr60 (A), Tyr398 (A), Leu171 (A), Tyr435 (A), Phe168 (A)	23.53%
ZINC000001530568, ZINC000001530567	DB00195	Betaxolol	4PQE	AChE	-7.9	-0.36	Tyr124 (A), Phe338 (A), Trp286 (A), Gly122 (A), Asp74 (A), Tyr341 (A), Ser203 (A), Gly121 (A), Tyr337 (A), Trp86 (A), Phe297 (A)	50.0%
			4BDT	AChE	-8.17	-0.37	Tyr124 (A), Phe338 (A), Thr83 (A), Gly122 (A), Asp74 (A), Phe295 (A), Ser203 (A), His447 (A), Trp439 (A), Gly121 (A), Tyr337 (A), Trp86 (A), Phe297 (A)	87.5%
			1ACJ	AChE	-8.01	-0.36	Ser122 (A), Gly123 (A), Trp84 (A), Asp72 (A), Phe330 (A), Tyr70 (A), Tyr334 (A)	20.0%
			1FKN	BACE1	-7.43	-0.34	Thr72 (A), Ala5 (C), Leu30 (A), Asn3 (C), Asp32 (A), Tyr71 (A), Gln73 (A), Val2 (C), Lys107 (A), Trp115 (A), Tyr198 (A), Val332 (A)	55.56%
			1P0P	BuChE	-7.35	-0.33	Tyr332 (A), Trp82 (A), Phe329 (A)	50.0%
			1UV5	GSK-3β	-7.02	-0.32	Val70 (A), Tyr134 (A), Leu132 (A), Leu188 (A), Ala83 (A), Asp200 (A), Lys85 (A), Val135 (A), Ile62 (A)	33.33%
			4A79	MAO-B	-8.02	-0.36	Trp119 (A), Ile316 (A), Tyr326 (A), Ile199 (A), Gln206 (A), Leu164 (A), Phe343 (A), Phe168 (A), Tyr398 (A), Leu171 (A), Tyr435 (A)	9.09%
			1GOS	MAO-B	-8.06	-0.37	Tyr326 (A), Ile199 (A), Gln206 (A), Phe343 (A), Tyr398 (A), Leu171 (A), Tyr435 (A)	17.65%
ZINC000001530569	DB00612	Bisoprolol	4PQE	AChE	-7.79	-0.34	Phe338 (A), Trp286 (A), Gly122 (A), Asp74 (A), Glu202 (A), Tyr341 (A), Ser203 (A), Gly121 (A), Tyr337 (A), Trp86 (A), Phe297 (A)	50.0%
			4BDT	AChE	-8.43	-0.37	Tyr124 (A), Phe338 (A), Tyr341 (A), Asn87 (A), Ser203 (A), Gly121 (A), Tyr337 (A), Trp86 (A), Phe297 (A)	62.5%
			1ACJ	AChE	-7.54	-0.33	Trp279 (A), Ile439 (A), Ser122 (A), Tyr121 (A), Trp84 (A), Phe330 (A), Tyr70 (A)	40.0%
			1P0P	BuChE	-7.02	-0.31	Trp82 (A), Phe329 (A), Ser198 (A), Trp231 (A), Leu286 (A)	50.0%
			3POZ	EGFR	-7	-0.3	Leu844 (A), Leu792 (A), Leu777 (A), Phe856 (A), Lys745 (A), Met766 (A), Leu718 (A), Met793 (A), Asp855 (A), Val726 (A), Thr790 (A), Thr854 (A)	55.56%
			4A79	MAO-B	-7.99	-0.35	Trp119 (A), Tyr326 (A), Ile199 (A), Ile198 (A), Gln206 (A), Leu164 (A), Phe343 (A), Tyr60 (A), Tyr398 (A), Leu171 (A), Tyr435 (A), Phe168 (A)	13.64%
			1GOS	MAO-B	-7.85	-0.34	Met436 (A), Gln206 (A), Tyr398 (A), Leu171 (A), Tyr435 (A)	17.65%

Table 4. Continued...

ZINC ID	DrugBank ID	Drug Name	Target PDB	Target Name	BE	LE	Interactions	PLIF Tanimoto
ZINC000000897251	DB00843	Donepezil	4PQE	AChE	-8.56	-0.31	Tyr124 (A), Phe338 (A), Trp286 (A), Tyr341 (A), Ser203 (A), Tyr337 (A), Trp86 (A), Phe297 (A)	50.0%
			4BDT	AChE	-8.91	-0.32	Asp74 (A), Ser125 (A), Tyr133 (A), Tyr449 (A), Trp439 (A), Pro446 (A), Tyr337 (A), Trp86 (A)	37.5%
			1ACJ	AChE	-8.5	-0.3	Trp279 (A), Tyr121 (A), Trp84 (A), Phe330 (A), Tyr70 (A), Tyr334 (A)	60.0%
			2QP8	BACE1	-8.78	-0.31	Asp93 (A), Gln134 (A), Tyr132 (A), Ile171 (A), Leu91 (A), Thr293 (A), Trp176 (A), Thr133 (A), Phe169 (A), Ile179 (A)	60.0%
			5HU1	BACE1	-8.55	-0.31	Asp93 (A), Ile287 (A), Tyr132 (A), Leu91 (A), Thr293 (A), Trp176 (A), Ile179 (A)	28.57%
			5I3V	BACE1	-8.98	-0.32	Phe108 (A), Leu30 (A), Asp32 (A), Tyr71 (A), Ile118 (A), Val69 (A)	45.45%
			2WJO	BACE1	-8.57	-0.31	Ile226 (A), Asp228 (A), Phe108 (A), Asp32 (A), Tyr71 (A), Val69 (A), Tyr198 (A), Val332 (A)	60.0%
			1P0P	BuChE	-9.43	-0.34	Phe329 (A), Ser198 (A), Gly117 (A), His438 (A), Asp70 (A), Gly116 (A), Tyr332 (A)	50.0%
			3POZ	EGFR	-9.48	-0.34	Leu844 (A), Leu777 (A), Phe856 (A), Lys745 (A), Met766 (A), Ala743 (A), Leu718 (A), Val726 (A), Thr790 (A)	33.33%
			1UV5	GSK-3β	-8.53	-0.3	Val70 (A), Tyr134 (A), Leu132 (A), Leu188 (A), Ala83 (A), Asp200 (A), Lys85 (A), Ile62 (A)	25.0%
			1GOS	MAO-B	-10.59	-0.38	Ala439 (A), Ser59 (A), Thr426 (A), Ile14 (A), Gln206 (A), Tyr60 (A), Tyr398 (A), Tyr435 (A)	29.41%
			5ES1	MARK4	-8.72	-0.31	Val70 (A), Tyr134 (A), Leu185 (A), Ala135 (A), Lys64 (A), Ala195 (A), Ile62 (A), Asp196 (A), Val116 (A)	57.14%
ZINC000003812841	DB00227	Lovastatin	4PQE	AChE	-9.22	-0.32	Tyr124 (A), Phe338 (A), Asp74 (A), Phe295 (A), Tyr341 (A), Ser125 (A), Leu130 (A), Trp439 (A), Tyr337 (A), Trp86 (A), Phe297 (A)	25.0%
			4BDT	AChE	-9.02	-0.31	Tyr124 (A), Phe338 (A), Thr83 (A), Asp74 (A), Phe295 (A), Tyr341 (A), Ser203 (A), Leu130 (A), Tyr133 (A), Trp439 (A), Tyr337 (A), Trp86 (A), Phe297 (A)	75.0%
			5I3V	BACE1	-8.97	-0.31	Phe108 (A), Leu30 (A), Arg128 (A), Tyr71 (A), Asn37 (A), Trp76 (A), Ser36 (A), Trp115 (A)	36.36%
			1P0P	BuChE	-9.61	-0.33	Trp82 (A), Phe329 (A), Ala328 (A), Thr120 (A), Tyr332 (A), Glu197 (A)	50.0%
			3POZ	EGFR	-9.04	-0.31	Leu844 (A), Leu792 (A), Lys745 (A), Leu718 (A), Val726 (A), Thr790 (A)	22.22%
			1UV5	GSK-3β	-9.01	-0.31	Val70 (A), Tyr134 (A), Leu132 (A), Leu188 (A), Lys85 (A), Thr138 (A)	8.33%
			4A79	MAO-B	-8.96	-0.31	Lys296 (A), Arg42 (A), Gln206 (A), Val294 (A), Phe343 (A), Tyr398 (A), Leu171 (A), Tyr435 (A)	13.64%
			1GOS	MAO-B	-10.87	-0.37	Lys296 (A), Arg42 (A), Gln206 (A), Val294 (A), Phe343 (A), Tyr60 (A), Tyr398 (A), Tyr435 (A)	17.65%
			5ES1	MARK4	-8.84	-0.3	Tyr134 (A), Leu185 (A), Ala83 (A), Glu139 (A), Lys85 (A), Ala68 (A), Glu182 (A), Ile62 (A), Gly65 (A)	57.14%

Table 4. Continued...

ZINC ID	DrugBank ID	Drug Name	Target PDB	Target Name	BE	LE	Interactions	PLIF Tanimoto
ZINC000000537822	DB00502	Haloperidol	4PQE	AChE	-9.6	-0.37	Phe338 (A), Trp286 (A), Asp74 (A), Tyr341 (A), Ser293 (A), Tyr337 (A), Trp86 (A)	25.0%
			4BDT	AChE	-8.62	-0.33	Asp74 (A), Tyr341 (A), Tyr449 (A), Trp439 (A), Tyr337 (A), Trp86 (A)	50.0%
			1ACJ	AChE	-8.86	-0.34	Trp279 (A), Tyr121 (A), Trp84 (A), Asp72 (A), Phe330 (A), Tyr70 (A), Tyr334 (A)	60.0%
			2QP8	BACE1	-9.03	-0.35	Asp93 (A), Gln134 (A), Tyr132 (A), Leu91 (A), Val130 (A), Thr133 (A), Phe169 (A), Asp289 (A), Asn98 (A), Thr292 (A), Ile187 (A), Tyr259 (A), Ile179 (A)	70.0%
			1FKN	BACE1	-7.84	-0.3	Phe108 (A), Ile110 (A), Asn111 (A), Asp32 (A), Tyr71 (A), Gln73 (A), Ile118 (A), Phe109 (A), Val2 (C), Trp115 (A)	44.44%
			5HU1	BACE1	-8.14	-0.31	Ser290 (A), Ile171 (A), Gln134 (A), Tyr132 (A), Leu91 (A), Tyr259 (A)	28.57%
			5I3V	BACE1	-8.54	-0.33	Leu30 (A), Asp32 (A), Tyr71 (A), Asn37 (A), Ile118 (A), Tyr14 (A), Trp76 (A), Val69 (A), Gly230 (A)	36.36%
			2WJO	BACE1	-8.2	-0.32	Ile110 (A), Leu30 (A), Thr232 (A), Gly11 (A), Gln12 (A), Val170 (A), Lys107 (A), Trp115 (A), Gly13 (A)	10.0%
			1P0P	BuChE	-9.22	-0.35	Trp82 (A), Phe329 (A), Ala328 (A), Asp70 (A), Thr120 (A)	50.0%
			3POZ	EGFR	-9.3	-0.36	Leu844 (A), Lys745 (A), Ala743 (A), Leu718 (A), Met793 (A), Asn842 (A), Val726 (A), Cys797 (A), Gln791 (A), Thr790 (A), Thr854 (A)	44.44%
			1UV5	GSK-3β	-9.13	-0.35	Val70 (A), Leu188 (A), Ala83 (A), Asp200 (A), Thr138 (A), Ile62 (A), Gln185 (A)	25.0%
			4A79	MAO-B	-11.15	-0.43	Ala35 (A), Tyr393 (A), Leu268 (A), Thr43 (A), Ile264 (A), Ala439 (A), Val235 (A), Thr426 (A), Ile14 (A), Ser15 (A), Glu34 (A), Gly13 (A)	36.36%
			1GOS	MAO-B	-10.87	-0.42	Ala35 (A), Ala439 (A), Tyr393 (A), Ile264 (A), Thr426 (A), Ile14 (A), Ser15 (A), Glu34 (A), Gly12 (A)	29.41%
			5K4I	MAPK1	-8.35	-0.32	Ile56 (A), Lys54 (A), Ile31 (A), Leu156 (A), Tyr36 (A), Met108 (A)	44.44%
			5ES1	MARK4	-8.14	-0.31	Val70 (A), Ala135 (A), Leu185 (A), Ala83 (A), Glu139 (A), Ala195 (A), Ile62 (A), Asp196 (A), Val116 (A)	71.43%
ZINC000019364222	DB00557	Hydroxyzine	4PQE	AChE	-8.07	-0.31	Tyr124 (A), Phe338 (A), Asp74 (A), Tyr341 (A), Tyr337 (A), Trp86 (A), Phe297 (A)	25.0%
			4BDT	AChE	-9.37	-0.36	Tyr124 (A), Asp74 (A), Gly120 (A), Ser203 (A), Tyr133 (A), Tyr449 (A), Trp439 (A), Glu202 (A), Tyr337 (A), Trp86 (A)	50.0%
			1ACJ	AChE	-9.25	-0.36	Trp432 (A), Tyr121 (A), Trp84 (A), Asp72 (A), Phe330 (A), Tyr70 (A), Tyr334 (A), Ser200 (A)	40.0%
			5HU1	BACE1	-7.87	-0.3	Gln134 (A), Thr390 (A), Tyr132 (A), Ser389 (A), Asp289 (A), Arg296 (A)	42.86%
			5I3V	BACE1	-8.35	-0.32	Phe108 (A), Asp32 (A), Tyr71 (A), Asn37 (A), Ile118 (A), Tyr14 (A), Val31 (A), Val69 (A)	36.36%
			1P0P	BuChE	-8.11	-0.31	Trp82 (A), Phe329 (A)	50.0%
			1UV5	GSK-3β	-8.09	-0.31	Val70 (A), Tyr134 (A), Leu132 (A), Leu188 (A), Ala83 (A), Asn64 (A), Lys85 (A), Ile62 (A)	25.0%
			4A79	MAO-B	-8.01	-0.31	Met436 (A), Lys296 (A), Phe343 (A), Tyr60 (A), Tyr398 (A)	9.09%
			1GOS	MAO-B	-10.24	-0.39	Phe343 (A), Tyr398 (A), Tyr435 (A), Arg42 (A)	11.76%

Table 4. Continued...

ZINC ID	DrugBank ID	Drug Name	Target PDB	Target Name	BE	LE	Interactions	PLIF Tanimoto
ZINC000005456939	DB00755	Tretinoin	4PQE	AChE	-9.33	-0.42	Tyr124 (A), Phe338 (A), Trp286 (A), Asp74 (A), Tyr341 (A), Ser125 (A), Val294 (A), Tyr337 (A), Trp86 (A)	25.0%
			4BDT	AChE	-7.61	-0.35	Tyr124 (A), Asp74 (A), Trp439 (A), Tyr337 (A), Trp86 (A)	37.5%
			1ACJ	AChE	-10.77	-0.49	Ile287 (A), Trp279 (A), Phe290 (A), Ser122 (A), Tyr121 (A), Trp84 (A), Phe331 (A), Phe330 (A), Tyr70 (A), Tyr334 (A)	60.0%
			2QP8	BACE1	-8.7	-0.4	Ile171 (A), Gln134 (A), Tyr132 (A), Thr390 (A), Thr133 (A), Val393 (A), Phe169 (A), Arg296 (A), Tyr259 (A), Ile179 (A)	40.0%
			5HU1	BACE1	-7.92	-0.36	Ile287 (A), Gln134 (A), Tyr132 (A), Thr390 (A), Phe169 (A), Arg296 (A), Tyr259 (A), Ile179 (A)	42.86%
			5I3V	BACE1	-7.93	-0.36	Phe108 (A), Ile110 (A), Leu30 (A), Thr232 (A), Tyr71 (A), Ile118 (A), Trp115 (A)	63.64%
			2FDP	BACE1	-7.54	-0.34	Ile110 (A), Leu30 (A), Tyr71 (A), Gln73 (A), Ile118 (A), Lys107 (A), Trp115 (A)	75.0%
			2WJO	BACE1	-8.15	-0.37	Phe108 (A), Ile126 (A), Ser35 (A), Tyr71 (A), Asn37 (A), Ser36 (A)	20.0%
			4DJU	BACE1	-7.99	-0.36	Ile171 (A), Tyr132 (A), Leu91 (A), Thr293 (A), Trp176 (A), Phe169 (A)	50.0%
			2OHU	BACE1	-7.34	-0.33	Ile110 (A), Arg128 (A), Tyr71 (A), Asn37 (A), Ile118 (A), Val69 (A), Trp115 (A)	44.44%
			1P0P	BuChE	-8.53	-0.39	Tyr332 (A), Trp82 (A), Phe329 (A)	50.0%
			3POZ	EGFR	-8.69	-0.4	Leu844 (A), Leu788 (A), Leu777 (A), Lys745 (A), Ala743 (A), Leu718 (A), Met793 (A), Asp855 (A), Thr790 (A), Thr854 (A)	55.56%
			1UV5	GSK-3β	-8.87	-0.4	Val70 (A), Tyr134 (A), Leu188 (A), Ala83 (A), Asp200 (A), Lys85 (A), Val110 (A), Ile62 (A), Thr138 (A), Arg141 (A)	33.33%
			4A79	MAO-B	-10.15	-0.46	Tyr326 (A), Arg42 (A), Ile198 (A), Tyr60 (A), Tyr398 (A), Leu171 (A), Tyr435 (A)	18.18%
			1GOS	MAO-B	-9.57	-0.43	Ala439 (A), Arg42 (A), Thr426 (A), Ile14 (A), Ser15 (A), Tyr398 (A), Tyr435 (A)	29.41%
			1PME	MAPK1	-7.63	-0.35	Lys54 (A), Val39 (A), Thr105 (A), Ala52 (A), Ile84 (A), Leu156 (A)	66.67%
			5K4I	MAPK1	-9.1	-0.41	Ile56 (A), Val39 (A), Tyr36 (A), Lys54 (A)	22.22%
			5ES1	MARK4	-8.07	-0.37	Val70 (A), Tyr134 (A), Leu185 (A), Lys85 (A), Ala68 (A), Ala195 (A), Ile62 (A), Asp196 (A)	57.14%
ZINC000002015928	DB01048	Abacavir	4PQE	AChE	-7.99	-0.38	Tyr124 (A), Thr83 (A), Asp74 (A), Gly120 (A), Tyr341 (A), Tyr337 (A), Trp86 (A)	25.0%
			4BDT	AChE	-8.79	-0.42	Tyr341 (A), Tyr133 (A), His447 (A), Tyr449 (A), Trp439 (A), Pro446 (A), Tyr337 (A), Trp86 (A)	50.0%
			1ACJ	AChE	-8.39	-0.4	His440 (A), Ile439 (A), Trp432 (A), Tyr130 (A), Gly117 (A), Tyr442 (A), Ser124 (A), Trp84 (A), Asp72 (A), Phe330 (A), Tyr334 (A)	20.0%
			2QP8	BACE1	-8.03	-0.38	Asp93 (A), Ile287 (A), Gly95 (A), Tyr132 (A), Gly291 (A), Thr133 (A), Val393 (A), Asp289 (A), Thr292 (A), Ile187 (A), Tyr259 (A)	60.0%
			5HU1	BACE1	-7.51	-0.36	Asp93 (A), Lys168 (A), Ile171 (A), Gln134 (A), Tyr132 (A), Gly291 (A), Ser96 (A), Phe169 (A), Asp289 (A), Ile179 (A)	85.71%
			5I3V	BACE1	-7.09	-0.34	Asp228 (A), Phe108 (A), Leu30 (A), Asp32 (A), Tyr71 (A)	27.27%
			2FDP	BACE1	-7.27	-0.35	Asp228 (A), Thr231 (A), Leu30 (A), Thr232 (A), Tyr71 (A), Ile118 (A), Lys107 (A), Gly230 (A)	50.0%
			2WJO	BACE1	-7.16	-0.34	Phe108 (A), Gly34 (A), Asp32 (A), Tyr71 (A), Lys107 (A), Gly230 (A), Tyr198 (A)	50.0%
			4DJU	BACE1	-7.5	-0.36	Ile171 (A), Tyr132 (A), Leu91 (A), Trp176 (A), Val130 (A), Gly291 (A), Phe169 (A)	66.67%
			1P0P	BuChE	-7.99	-0.38	Trp82 (A), Ser198 (A), His438 (A), Thr120 (A), Leu286 (A)	100.0%
			3POZ	EGFR	-8.16	-0.39	Leu844 (A), Leu788 (A), Leu777 (A), Lys745 (A), Ala743 (A), Asn842 (A), Asp855 (A), Val726 (A), Thr790 (A)	33.33%
			1UV5	GSK-3β	-7.51	-0.36	Leu132 (A), Leu188 (A), Asp200 (A), Lys85 (A), Val110 (A), Pro136 (A), Thr138 (A), Ile62 (A), Gln185 (A)	41.67%
			4A79	MAO-B	-8.5	-0.4	Ala35 (A), Tyr393 (A), Leu268 (A), Ile264 (A), Ala439 (A), Arg42 (A), Arg36 (A), Ala263 (A), Gly13 (A)	18.18%
			1GOS	MAO-B	-9.44	-0.45	Ala35 (A), Tyr393 (A), Val235 (A), Arg42 (A), Arg36 (A), Ala263 (A), Gly41 (A), Glu34 (A)	23.53%
			1PME	MAPK1	-7.67	-0.36	Glu71 (A), Lys54 (A), Thr105 (A), Ile84 (A), Leu156 (A), Leu103 (A), Met108 (A)	66.67%
			5K4I	MAPK1	-7.19	-0.34	Asn154 (A), Asp106 (A), Lys54 (A), Val39 (A), Ala52 (A), Asp167 (A), Asp111 (A), Leu156 (A), Met108 (A)	66.67%
			5ES1	MARK4	-7.57	-0.36	Val70 (A), Ala83 (A), Glu139 (A), Lys85 (A), Glu182 (A), Val116 (A)	42.86%

Table 4. Continued...

ZINC ID	DrugBank ID	Drug Name	Target PDB	Target Name	BE	LE	Interactions	PLIF Tanimoto
ZINC000000538312	DB00734	Risperidone	4PQE	AChE	-10.91	-0.36	Tyr124 (A), Phe338 (A), Trp286 (A), Tyr341 (A), Ser125 (A), Ser203 (A), His447 (A), Tyr72 (A), Tyr337 (A), Trp86 (A), Phe297 (A)	75.0%
			4BDT	AChE	-9.32	-0.31	Tyr124 (A), Thr83 (A), Asp74 (A), Tyr341 (A), Tyr449 (A), Trp439 (A), Tyr337 (A), Trp86 (A)	62.5%
			1ACJ	AChE	-10.67	-0.36	Trp279 (A), Ile287 (A), Glu199 (A), Ser122 (A), Tyr121 (A), Trp84 (A), Asp72 (A), Tyr70 (A), Tyr334 (A)	60.0%
			2QP8	BACE1	-9.34	-0.31	Asp93 (A), Ile287 (A), Ile171 (A), Gln134 (A), Tyr132 (A), Leu91 (A), Thr390 (A), Trp176 (A), Val393 (A), Phe169 (A), Asp289 (A), Thr292 (A), Tyr259 (A)	60.0%
			5HU1	BACE1	-10.4	-0.35	Asp93 (A), Ile287 (A), Gln134 (A), Tyr132 (A), Thr390 (A), Val393 (A), Phe169 (A), Asp289 (A), Arg296 (A), Tyr259 (A), Ile179 (A)	71.43%
			5I3V	BACE1	-10.28	-0.34	Phe108 (A), Leu30 (A), Ser35 (A), Asp32 (A), Tyr71 (A), Ile118 (A)	36.36%
			2WJO	BACE1	-9.12	-0.3	Phe108 (A), Asp32 (A), Thr329 (A), Tyr71 (A), Ile118 (A), Tyr198 (A), Val332 (A)	50.0%
			4DJU	BACE1	-10.03	-0.33	Asp93 (A), Lys168 (A), Ile171 (A), Tyr132 (A), Val130 (A), Phe169 (A), Asn98 (A)	66.67%
			1P0P	BuChE	-11.26	-0.38	Trp82 (A), Phe329 (A), Pro285 (A), Asp70 (A), Thr120 (A), Trp430 (A), Tyr332 (A), Leu286 (A)	50.0%
			3POZ	EGFR	-10.12	-0.34	Leu844 (A), Phe997 (A), Lys745 (A), Met766 (A), Leu718 (A), Asp855 (A), Thr790 (A)	33.33%
			1UV5	GSK-3β	-10.39	-0.35	Val70 (A), Tyr134 (A), Leu132 (A), Leu188 (A), Ala83 (A), Lys85 (A), Val110 (A), Ile62 (A), Arg141 (A), Asp133 (A)	25.0%
			4A79	MAO-B	-12.37	-0.41	Ala35 (A), Ala439 (A), Leu268 (A), Thr43 (A), Ile264 (A), Tyr393 (A), Arg42 (A), Thr426 (A), Ile14 (A), Glu34 (A), Lys271 (A), Gly13 (A)	31.82%
			1GOS	MAO-B	-12.04	-0.4	Ala439 (A), Tyr326 (A), Arg42 (A), Thr426 (A), Gln206 (A), Phe343 (A), Tyr398 (A), Leu171 (A)	29.41%
			1PME	MAPK1	-9.2	-0.31	Glu71 (A), Ile56 (A), Arg67 (A), Val39 (A), Ala52 (A), Asp167 (A), Leu156 (A), Tyr36 (A)	50.0%
			5K4I	MAPK1	-10.83	-0.36	Ile56 (A), Ile31 (A), Val39 (A), Ala52 (A), Asp167 (A), Asp111 (A), Leu156 (A), Tyr36 (A)	55.56%
			5ES1	MARK4	-9.16	-0.31	Val70 (A), Tyr134 (A), Ala135 (A), Leu185 (A), Ala83 (A), Gly138 (A), Lys85 (A), Glu133 (A), Ile62 (A), Met132 (A), Val116 (A)	57.14%
ZINC000001552908	DB06702	Fesoterodine	4PQE	AChE	-9.53	-0.32	Tyr124 (A), Phe338 (A), Gly120 (A), Ser203 (A), His447 (A), Tyr449 (A), Trp439 (A), Tyr337 (A), Trp86 (A), Phe297 (A)	75.0%
			1GOS	MAO-B	-9.07	-0.3	Gln206 (A), Gly57 (A), Phe343 (A), Tyr60 (A), Tyr398 (A), Tyr435 (A)	11.76%
ZINC000035024346	DB00121	Biotin	4BDT	AChE	-7.33	-0.46	Tyr124 (A), Gly122 (A), Ser203 (A), Gly121 (A), Tyr337 (A), Trp86 (A)	62.5%
			4A79	MAO-B	-7.18	-0.45	Met436 (A), Ser59 (A), Gln206 (A), Tyr60 (A), Tyr398 (A), Tyr435 (A)	18.18%
			1GOS	MAO-B	-7.94	-0.5	Val10 (A), Ala35 (A), Tyr393 (A), Ile264 (A), Val235 (A), Arg36 (A), Glu34 (A)	17.65%

Table 4. Continued...

ZINC ID	DrugBank ID	Drug Name	Target PDB	Target Name	BE	LE	Interactions	PLIF Tanimoto
ZINC000001546066	DB00530	Erlotinib	4PQE	AChE	-8.92	-0.31	Tyr124 (A), Phe338 (A), Trp286 (A), Gly82 (A), Asp74 (A), Tyr341 (A), Ser203 (A), Tyr72 (A), Trp86 (A)	25.0%
			4BDT	AChE	-9.16	-0.32	Thr83 (A), Gly122 (A), Tyr341 (A), Asn87 (A), Ser125 (A), Ser203 (A), Tyr133 (A), Tyr449 (A), Trp439 (A), Gly121 (A), Tyr337 (A), Trp86 (A)	100.0%
			1ACJ	AChE	-9.21	-0.32	Trp279 (A), Gly119 (A), Ser122 (A), Trp84 (A), Phe331 (A), Asp72 (A), Phe330 (A), Tyr70 (A), Tyr334 (A), Ser200 (A)	40.0%
			1P0P	BuChE	-8.98	-0.31	Trp82 (A), Phe329 (A), Ser198 (A), Ala328 (A), Gly117 (A), Asp70 (A), Asn83 (A), Tyr332 (A)	50.0%
			4A79	MAO-B	-9.13	-0.31	Tyr326 (A), Gln206 (A), Phe343 (A), Tyr60 (A), Tyr398 (A), Leu171 (A), Tyr435 (A)	13.64%
			1GOS	MAO-B	-9.32	-0.32	Met436 (A), Leu328 (A), Tyr326 (A), Gln206 (A), Phe343 (A), Tyr60 (A), Tyr398 (A)	23.53%

Discussion

QSAR modelling and virtual screening

This study employed a robust in silico screening approach combining QSAR modeling, virtual screening, and molecular docking to identify potential multi-target drugs for Alzheimer's Disease (AD) from a library of FDA-approved compounds. This strategy leverages the power of bioinformatics to accelerate drug discovery and repurposing, addressing the complex and multi-faceted nature of AD.

The QSAR models developed in this study demonstrated varying degrees of predictive performance, as indicated by the F1-scores and accuracy metrics. The consistent selection of the Extremely Randomized Tree (ET) algorithm across most bioassays highlights its efficacy in handling diverse datasets and complex relationships between molecular descriptors and biological activity. ET, as an ensemble method, is known for its robustness against overfitting and ability to capture non-linear relationships, making it suitable for predicting activity against multiple AD targets. The utilization of Morgan fingerprints as molecular descriptors further underscores the importance of molecular substructures in determining the activity of compounds against these targets. The varying F1-scores (57.12 to 88.08) reflect the inherent differences in the complexity and quality of the PubChem BioAssay datasets. Datasets with higher F1-scores likely had clearer structure-activity relationships, while those with lower scores may have had more noise or less defined boundaries between active and inactive compounds.

The assessment of the Applicability Domain (AD) was crucial for ensuring the reliability of the model predictions. The Kernel Density method, being more nuanced than the Convex Hull method, provided a more accurate representation of the chemical space covered by the training data. The observation that no FDA molecules fell outside the AD using the Kernel Density method indicates that the predictions for these compounds are likely to be reliable. This is a significant finding, as it validates the use of these QSAR models for screening FDA-approved drugs. The slight deviations observed with the Convex Hull method suggest that while most FDA molecules are well within the training data's chemical space, a few may represent novel or underrepresented regions. This highlights the importance of using multiple AD assessment methods to gain a comprehensive understanding of the model's limitations and applicability.

The virtual screening process prioritized molecules with high BBB permeability and desirable predicted activities against multiple AD targets. The selection of 427 molecules, based on these criteria, significantly narrowed the search space and focused the subsequent docking studies on compounds with a higher likelihood of efficacy. The filtering out of PAINS compounds and those with undesirable ADMET properties further refined the selection, ensuring that the final list of candidates had a favorable profile for further development.

The molecular docking analysis provided valuable insights into the binding modes and interactions of the selected molecules with the AD targets. The stringent selection criteria for docking results ($\Delta G <= -7.0$ kcal/mol, ligand efficiency <= -0.3 kcal/mol) ensured that only high-affinity and efficient interactions were considered. The Protein-Ligand Interaction Fingerprint (PLIF) analysis, coupled with Tanimoto similarity scores, enabled the evaluation of the predicted binding modes' relevance to known mechanisms of action. High Tanimoto scores indicate that the predicted binding interactions closely match those described in the literature for known active compounds, further validating the docking results. The identification of the top 20 molecules, based on their docking scores and PLIF analysis, provides a prioritized list of candidates for further experimental validation. The multi-target nature of these molecules, as evidenced by their interactions with multiple AD targets, makes them particularly promising for addressing the complex pathophysiology of the disease.

Molecular targets

Beta-site amyloid precursor protein cleaving enzyme 1 (BACE1) is responsible for the cleavage of the amyloid-ß peptides, including the Aß42, which is the main component of extracellular amyloid plaques. BACE1 also plays a role in synaptic plasticity and homeostasis (Das & Yan, 2017); consequently, many clinical trials for inhibitors have been discontinued due to safety concerns. Nevertheless, BACE1 remains a crucial molecular target for AD (Hampel et al., 2021). Binders to the Aß42 peptide were also evaluated as potential drugs for AD, as Aß42 also interacts with other proteins in the brain, including the cellular prion protein (PrP^c), which might be associated with cognitive impairment in the late stages of AD (Grayson et al., 2021).

Tau is a microtubule-associated protein responsible for maintaining the structural stability of the microtubules inside the neuron. During AD, however, the protein accumulates inside the cell, forming insoluble filaments, primarily due to abnormal hyperphosphorylation by an array of kinases (Muralidar et al., 2020). The triggering of Tau hyperphosphorylation may be associated with the accumulation of amyloid outside the cell, which leads to neuroinflammation and activates different kinase pathways, including the MAPK. Other kinases related to this process are GSK3, MARK, cAMP-dependent protein kinase (PKA), and many Cyclin-dependent Kinases (CDKs) (Medeiros et al., 2011). Tau dephosphorylation is performed by phosphatases such as PP2A, but the expression of this enzyme is inhibited by the gene SET, which contains a functional kB site in its promoter.

NF-kB is a redox-sensitive transcription factor and a major regulator of inflammation in different physiological contexts. In AD, particularly, it induces the expression of proinflammatory cytokines, such as IL-1, IL-6, and TNF-α by microglia and astrocytes, which damages the myelin in oligodendrocytes, making the neuron more vulnerable to the toxic effect of amyloid peptides. The expression of NF-kB is induced by the presence of danger-associated molecular patterns (DAMPs) and amyloid peptides (Ju Hwang et al., 2019). NF-κB also regulates the expression of apolipoprotein E (APOE), and some variants of this protein are associated with the inhibition of amyloid peptide clearance in the extracellular space, thereby increasing the risk of AD (Raulin et al., 2022).

Acetylcholine is a neurotransmitter secreted by cholinergic neurons and is highly associated with memory and learning functions (Mashour, 2011). During AD, there is a reduction in the cholinergic activity in the brain, which is related to the cognitive decline observed during the disease progression. The cholinergic system comprises muscarinic (mAChR) and nicotinic acetylcholine receptors (nAChR), each of which is a family of signaling membrane proteins. Although the role of nAChRs during AD is less understood, it's well-known that Aß peptides interact with nAChRs, particularly with the α7 subunit. However, the effect of this interaction (inhibition or activation) is still debated; however, higher concentrations of Aß are more associated with the inhibition of the receptors (Lombardo & Maskos, 2015).

Finally, monoamine Oxidase (MAO) is an enzyme present in two forms (A and B), encoded by different genes and with distinct tissue distributions. MAO-B is the main form present in the brain, and it's associated with the oxidation of monoamine neurotransmitters, which leads to the liberation of reactive oxygen species (ROS), such as hydrogen peroxide (H_2O_2) (Manzoor & Hoda, 2020). Oxidative stress leads to neuroinflammation and the formation of amyloid plaques, a primary characteristic of AD (Huang et al., 2016). Therefore, MAO inhibitors such as Rasagiline, currently used for Parkinson's Disease (PD), have been considered for the treatment of AD, demonstrating promising results in clinical trials (Matthews et al., 2021).

Psychotropic medications

Pimozide (Orap®) is a medication classified as an antipsychotic, indicated for the treatment of Tourette's Disorder and for the management of motor and phonic tics, which are characteristic of this syndrome. Its mechanism of action appears to lie in its ability as a dopaminergic blocker by binding to and inhibiting the dopamine D2 receptor in the CNS. Pimozide is capable of inducing mTOR-independent autophagy, but through an as yet unknown mechanism of action (Zhang et al., 2007), and of decreasing the formation of proteins in alpha-1-antitrypsin-deficient *C. elegans* (O'Reilly et al., 2016). Kim et al. (2016, 2017) demonstrated that pimozide induces AMPK-mediated autophagy but not mTOR-associated autophagy. Pimozide also decreases levels of tau oligomers and aggregates, rescuing memory deficits in a TauC3 mouse model (tau aggregation-prone mice) through increased autophagy. Based on the docking simulations, Pimozide demonstrated potential interactions with AChE (as previously suggested by Kumar et al. (2017), as well as with MAO-B, BuChE, BACE1, and MAPK1. The possible effect of pimozide as an antagonist of AchE was also demonstrated by the QSAR models generated by Bambu from the BioAssays 1347395 and 1347398, with a probability higher than 70% in both, along with a potential antagonistic effect on CHRM1, with a probability higher than 85%. However, Pimozide is, in fact, a potential agonist of CHRM1, as demonstrated by (Sutherland et al., 2023) in an HTS study available at PubChem BioAssays (BioAssay: 1961716). Additionally, the effect of Pimozide and other antipsychotics on the enhancement of the inhibition of AChE and BuChE by rivastigmine was recently demonstrated (Podsiedlik et al., 2022), suggesting a synergic effect.

Our molecular docking simulations reveal a compelling multi-target profile for Pimozide, suggesting potential interactions with key Alzheimer's Disease (AD)-related proteins. Notably, the strong binding affinity observed for Acetylcholinesterase (AChE, BE = -11.24 kcal/mol) suggests Pimozide may interact with residues in both the anionic site (e.g., Trp84, Phe330) and the peripheral anionic site (PAS, e.g., Trp279, Tyr334), potentially leading to potent inhibition through a combination of competitive and allosteric mechanisms. Additionally, the very strong binding to Monoamine Oxidase B (MAO-B, BE = -12.48 and -12.33 kcal/mol) indicates potential interactions with residues forming the aromatic cage (e.g., Tyr398, Tyr435) and those near the FAD cofactor, suggesting Pimozide could hinder substrate binding and/or disrupt the cofactor's redox activity, thereby reducing oxidative stress. The significant binding to Butyrylcholinesterase (BuChE, BE = -11.01 kcal/mol) further supports a cholinergic modulation role. The interaction with Beta-Secretase 1 (BACE1, BE = -10.37 kcal/mol) suggests Pimozide may

interfere with the catalytic dyad (e.g., Asp32) or the flap region, potentially inhibiting amyloid-beta production. Furthermore, the binding to MAPK1 (BE = -10.63 kcal/mol) hints at a possible role in modulating tau phosphorylation pathways.

Donepezil (Adlarity®) is a drug that acts as an acetylcholinesterase inhibitor, usually used in therapy to control the behavioral and cognitive symptoms that occur in AD. Donepezil can selectively and reversibly inhibit acetylcholinesterase, which is responsible for the decomposition of acetylcholine (DrugBank: DB00843). Donepezil is highly selective for acetylcholinesterase, with less selectivity for butyrylcholinesterase. It has a safe pharmacokinetic, pharmacodynamic, and toxicity profile, according to studies, and the drug demonstrates a significant ability to improve cognitive and global functions in patients with mild to moderate AD (Shigeta & Homma, 2001). Donepezil derivatives have already been demonstrated as potential multi-target drugs against AD, with inhibitory activity on AChE, BuChE, MAO-B, and MAO-A (Li et al., 2016).

Analysis of docking results not only reaffirms Donepezil's primary role as a potent Acetylcholinesterase (AChE) inhibitor, with strong binding affinities consistently observed across multiple AChE structures (BE = -8.50 to -8.91 kcal/mol), but also uncovers its significant potential as a multi-target agent. The simulations predict a very favorable interaction with Monoamine Oxidase B (MAO-B, BE = -10.59 kcal/mol), suggesting a secondary mechanism for reducing oxidative stress. Furthermore, Donepezil demonstrated strong affinity for Butyrylcholinesterase (BuChE, BE = -9.43 kcal/mol) and, notably, for Beta-Secretase 1 (BACE1), with consistent binding energies across several structures (BE = -8.57 to -8.98 kcal/mol). This suggests a potential to interfere with amyloid-beta production directly. The predicted binding to key kinases like GSK-3ß and MARK4 also hints at a possible role in modulating tau hyperphosphorylation pathways. This multi-target profile indicates that Donepezil's therapeutic benefits may be broader than just cholinergic enhancement, supporting its investigation as a more comprehensive AD treatment.

Risperidone (Perseris®) can treat schizophrenia, bipolar disorder, and psychosis, and it also acts as an adjuvant in managing depression. Risperidone inhibits dopaminergic D2 receptors, as well as serotonergic 5-HT2A receptors present in the brain (DrugBank: DB00734). Risperidone is indicated in some countries for the management of aggressive symptoms and psychosis in patients with severe dementia, where patients with AD are included (Davies et al., 2018). Finally, Risperidone was already proposed as a potential drug for AD treatment and evaluated in the treatment of psychosis associated with AD (Katz et al., 2007; Negrón & Reichman, 2000; Zeng et al., 2019), with positive results. The docking simulations revealed a firm multi-target profile, with a predicted binding affinity for Monoamine Oxidase B (MAO-B) that was among the highest in the study (BE = -12.37 kcal/mol), indicating a powerful potential to combat oxidative stress. Furthermore, Risperidone showed powerful interactions with both Butyrylcholinesterase (BuChE, BE = -11.26 kcal/mol) and Acetylcholinesterase (AChE, BE up to -10.91 kcal/mol), suggesting a robust ability to modulate the cholinergic system. Critically, it also demonstrated consistent, high-affinity binding to multiple BACE1 structures (BE up to -10.40 kcal/mol) and key tau-related kinases like GSK-3ß (BE = -10.39 kcal/mol) and MAPK1 (BE = -10.83 kcal/mol). This predicted ability to simultaneously engage with drivers of amyloid pathology, tau hyperphosphorylation, and oxidative stress makes Risperidone a standout candidate for further investigation as a comprehensive, disease-modifying therapy for AD.

Hypertension and antiarrhythmic medications

Ibutilide (Corvert®) is a class III antiarrhythmic drug used to correct atrial fibrillation and atrial flutter. The presentations of ibutilide found on the market today are intravenous. It can bind to and alter hERG potassium channels, delayed-entry rectifying potassium channels, and L-type calcium channels, which are sensitive to dihydropyridine (DrugBank: DB00308). To date, there is no indication in the literature of the use of Ibutilide for treating AD. Betaxolol (Betoptic®) is a beta-blocker used to treat hypertension or ocular hypertension (DrugBank, 2023). Its mechanism of action lies in the ability to selectively block catecholamine stimulation of ß-1-adrenergic receptors found in the heart and vascular smooth muscle (DrugBank: DB00195). Bisoprolol (Ziac®) is used to treat moderate hypertension and prevent myocardial infarction, also belonging to the class of ß-blockers. In a similar *in silico* screening study conducted by Fiscon and collaborators, they had already identified both betaxolol and bisoprolol as potential drugs for repositioning studies in the treatment of AD (Fiscon et al., 2022). Beta-blockers able to permeate the blood-brain barrier may be associated with a reduced risk of developing AD in patients using this class of medication to treat hypertension. The possible mechanism for this delay in the development of AD would occur through the more voluminous flow of cerebrospinal fluid driven by cardiac-arterial pulses, occurring in these patients with the help of medication, which would be capable of removing accumulations of ß-amyloid and tau protein, through the perivenous spaces and cranial nerves (Beaman et al., 2023).

While there is no previous indication for its use in Alzheimer's Disease, our in silico analysis identified Ibutilide as a promising candidate due to its predicted interactions with key AD targets. The molecular docking simulations showed that Ibutilide has a favorable binding affinity for both Acetylcholinesterase (AChE, BE = -8.12 kcal/mol) and Monoamine Oxidase B (MAO-B, BE up to -8.71 kcal/mol). Notably, its interaction with AChE achieved a high Protein-Ligand Interaction Fingerprint (PLIF) score of 40.0%, engaging with critical residues of the enzyme's active site gorge, including Trp84, Phe330, and Trp279. This suggests a strong potential to modulate the cholinergic system. The concurrent predicted binding to MAO-B indicates a possible secondary mechanism for reducing neurotoxic oxidative stress. This novel, dual-target profile makes Ibutilide an intriguing candidate for experimental validation to explore a previously unknown therapeutic avenue for AD.

Statins

Rosuvastatin (DrugBank: DB01098), Fluvastatin (DrugBank: DB01095), and Lovastatin (DrugBank: DB00227) are HMG-CoA reductase inhibitors from the statin class. Although early studies have indicated a potential negative impact on cognitive decline, more recent studies and further meta-analyses have suggested that statins might reduce cognitive decline.

Based on the docking results, the analyzed molecules presented a high affinity for acetylcholinesterase (AChE) and butyrylcholinesterase (BChE), which is in concordance with previous studies that demonstrated statins might downregulate the activity of these enzymes (Pytel et al., 2017).

Vitamins

The potential benefits of vitamin E (DrugBank: DB00163), alpha-tocopherol, have already been debated in the treatment of AD, as it might play a role in the reduction of oxidative stress and neuroinflammation, thus presenting a neuroprotective effect. Additionally, it's also known that the levels of vitamin E in the brain of people with AD are usually lower than those observed in people without the disorder. In our analysis, Vitamin E was found to have a potential interaction with AChE, as previously demonstrated by Thomé et al. (2011), and also with MAO-B. However, no direct interaction between MAO-B and Vitamin E has been presented. Biotin, another essential vitamin, was also identified as a potential binder to AChE and MAO-B, but no experimental description of possible interactions or biological effects is known for these targets, and no relation with AD is known for this molecule.

Specifically for Rosuvastatin, the docking analysis provides a detailed molecular rationale for this effect. Our results show a strong predicted binding affinity for Acetylcholinesterase (AChE), with a binding energy of -9.91 kcal/mol. The simulation suggests that Rosuvastatin forms an extensive network of interactions within the active site gorge of the enzyme. Notably, it is predicted to engage with key residues of both the catalytic anionic site (such as Trp84 and Phe330) and the catalytic triad (including Ser200 and Glu199). This comprehensive binding pattern, occupying a significant portion of the active site, provides a strong structural basis for its potential as an effective AChE inhibitor, supporting the hypothesis that its neuroprotective benefits may stem in part from direct modulation of the cholinergic system.

Incontinence medications

Darifenacin (Emselex) (DrugBank: DB00496) is a medication used to control urinary incontinence and is classified as an M3 muscarinic receptor blocker. The drug selectively antagonizes the M3 receptor, which is associated with functions such as bladder contraction, saliva production, and contraction of gastrointestinal smooth muscles (DrugBank: DB00496). Darifenacin has already been identified in another study screening potential new drugs for AD as a promising molecule (Hassan et al., 2023), but no relation to AD is known. Our *in silico* analysis provides a strong molecular rationale for Darifenacin's potential in Alzheimer's Disease, revealing a potent, multi-target profile. The docking simulations predicted a powerful binding affinity for Acetylcholinesterase (AChE), with a binding energy reaching as low as -12.05 kcal/mol, and a similarly powerful interaction with Butyrylcholinesterase (BuChE, BE = -10.71 kcal/mol). This suggests a robust capacity to modulate the cholinergic system. Beyond this, Darifenacin demonstrated powerful predicted affinities for Monoamine Oxidase B (MAO-B, BE up to -11.32 kcal/mol) and Beta-Secretase 1 (BACE1, BE up to -10.10 kcal/mol). This combination of predicted high-affinity interactions suggests that Darifenacin could simultaneously address cholinergic deficits, reduce oxidative stress, and inhibit amyloid-beta production, making it a highly compelling candidate for experimental validation in AD models.

Other drugs

Droperidol (Inapsine®) is a drug derived from butyrophenone, with dopamine antagonist action, mainly used to treat nausea and vomiting. Its exact mechanism of action is still considered unknown, but droperidol causes CNS depression at the subcortical levels of the brain, midbrain, and reticular formation of the brainstem. Furthermore, it exhibits intense central antidopaminergic action, as well as ganglionic blockade and a reduction in the affective response (DrugBank: DB00450). In another virtual screening study, droperidol was also demonstrated to be a potential therapeutic agent for AD, through the inhibition of the aggregation of the protein (Alabdulraheem & Durdagi, 2023). In an *in vitro* study, it was evaluated in combination with haloperidol and showed the ability to inhibit Aß peptides in cell cultures (Higaki et al., 1997, p. 7). Molecular docking analysis supports and expands upon previous findings, providing a detailed molecular framework for the potential of Droperidol as an Alzheimer's therapeutic. The docking analysis revealed exceptionally strong predicted binding affinities for key enzymes, most notably Acetylcholinesterase (AChE), with a binding energy as low as -11.38 kcal/mol. It also showed very potent interactions with Monoamine Oxidase B (MAO-B, BE = -11.27 kcal/mol), suggesting a dual capacity to address both cholinergic decline and oxidative stress. Furthermore, Droperidol's significant and consistent binding to multiple BACE1 structures (BE up to -9.38 kcal/mol) offers a direct molecular mechanism for the previously observed inhibition of Aß peptides. This predicted ability to simultaneously engage with the cholinergic system, oxidative stress pathways, and amyloid production makes Droperidol a high-priority, multi-target candidate for further investigation.

Perspectives

The identification of novel pharmaceutical applications for already approved molecules may boost the development of new treatments for a wide variety of diseases, not just Alzheimer's. *In silico* methods, such as molecular docking and QSAR, facilitate the screening of large libraries of molecules, reducing costs and allowing a more refined analysis in further *in vitro* and *in vivo* steps. Additionally, these methods might be used to explore potential interactions and mechanisms that are not easily observed *in vitro*, such as the interface of interaction between ligands and proteins. Additionally, considering the multifactorial nature of AD and the numerous hypotheses that might be used to understand the disease, multi-target drugs become a promising, albeit still unconventional, approach for treatment.

The screening of FDA-approved drugs allowed the identification of candidate molecules with potential activity against one or more molecular targets of AD. The possible activity of Pimozide, Donepezil, Bisoprolol, Ibutilide, Risperidone, Lovastatin, Rosuvastatin, Fluvastatin, Droperidol, Betaxolol, and Vitamin E (Figure 1) on AD or some of its

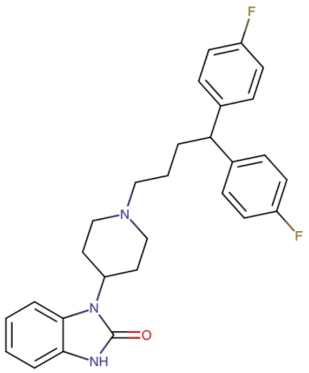

Pimozide
(ZINC000004175630)

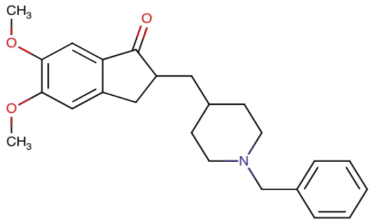

Donepezil
(ZINC000000897251)

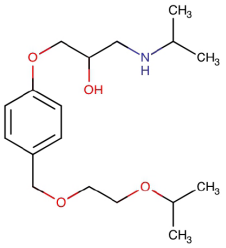

Bisoprolol
(ZINC000001530569)

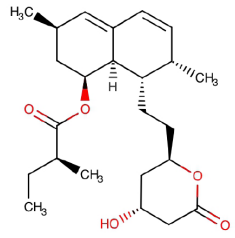

Lovastatin
(ZINC000003812841)

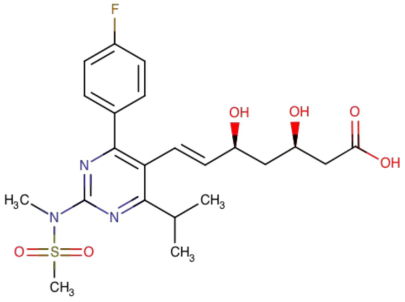

Rosuvastatin
(ZINC000001535101)

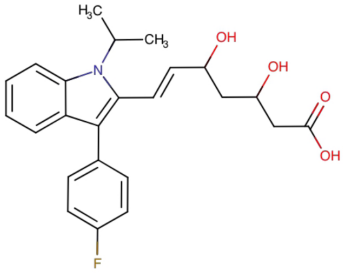

Fluvastatin
(ZINC000001886617)

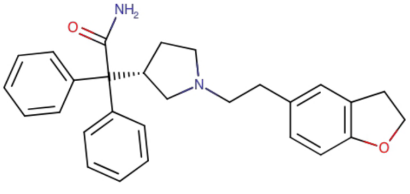

Darifenacin
(ZINC000001886617)

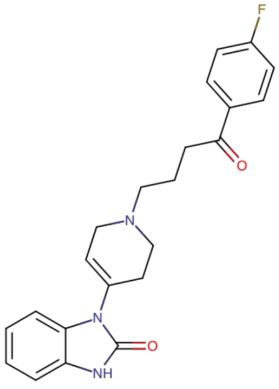

Droperidol
(ZINC000019796080)

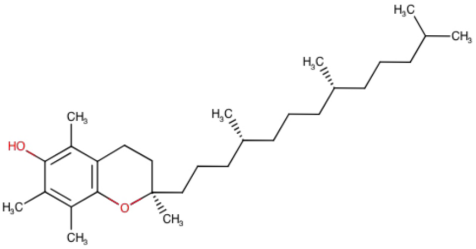

Vitamin E
(ZINC000004095858)

Figure 1. Candidates for drug repurposing were identified using QSAR and molecular docking from a dataset of FDA-approved drugs, with potential activity against Alzheimer's Disease molecular targets, as reported in the literature.

molecular targets, as supported by the literature, corroborates the *in silico* findings. Therefore, these molecules might be potential candidates for future *in vitro* and *in vivo* studies, and hit expansion might be employed to identify analog compounds with higher affinity to these particular molecular targets (Dolciami et al., 2024). Finally, the approach employed in the present work might be furtherly extended for larger libraries, using the entire ZINC database (ZINC, 2023), or the Enamine Database (Enamine, 2023), which provides a more concise and synthetically feasible collection of molecules.

Finally, several limitations of the current computational framework must be acknowledged. First, while the use of public HTS data enables large-scale modeling, it introduces inherent noise and assay heterogeneity that cannot be fully eliminated despite rigorous curation. Consequently, the QSAR models should be interpreted as probabilistic filters rather than definitive predictors of biological activity. Second, the use of random under-sampling to address class imbalance, while necessary for model convergence, likely yields performance metrics (e.g., F1-scores) that are optimistic relative to the low prevalence of active compounds in prospective screening scenarios. Third, our Applicability Domain assessment relies on UMAP embeddings; while this preserves the local manifold structure of the chemical space, it is a non-linear approximation that may distort global distance relationships compared to high-dimensional fingerprint spaces. Lastly, the strict probability thresholds and logical schema utilized were designed to maximize precision and safety, which inevitably reduces the recall rate, potentially excluding marginal but valid candidates. Therefore, all identified hits remain theoretical candidates that require definitive *in vitro* and *in vivo* validation to confirm their multi-target efficacy and safety profile.

Conclusion

This study has employed an integrated *in silico* approach, combining QSAR modeling, virtual screening, and molecular docking, to identify potential multi-target drug candidates for Alzheimer's Disease (AD) from a library of FDA-approved compounds. The rigorous assessment of the Applicability Domain validated the reliability of our predictions. Molecular docking studies provided detailed insights into the binding modes and interactions of selected molecules with key AD-related targets like AChE, BACE1, and MAO-B. Notably, molecules such as Droperidol and Pimozide demonstrated high predicted affinity for both AChE and BACE1, suggesting potential multi-target activity crucial for addressing the complex pathophysiology of AD. The Protein-Ligand Interaction Fingerprint (PLIF) analysis further supported these findings by evaluating the relevance of predicted binding modes to known mechanisms of action.

The top 20 molecules identified through this comprehensive *in silico* screening represent a prioritized list of candidates for further experimental validation. These FDA-approved molecules offer a significant advantage for potential repurposing, potentially accelerating the development of new AD therapies. By focusing on compounds with established safety profiles and known pharmacokinetic properties, we can potentially bypass lengthy and costly early-stage drug development phases. The multi-target nature of these molecules, interacting with various AD-related proteins, makes them particularly promising for addressing the multifaceted aspects of the disease.

While these *in silico* findings are promising, it is crucial to acknowledge their limitations. Computational predictions must be validated through rigorous *in vitro* and *in vivo* studies. Future research should focus on confirming the biological activity of the identified molecules, investigating their efficacy in preclinical AD models, and assessing potential off-target effects and toxicity. Additionally, exploring the synergistic effects of combining these molecules could be a valuable avenue for developing more effective therapeutic strategies. Finally, this study provides a robust computational framework for identifying multi-target drug candidates for AD and offers a strong foundation for future experimental investigations, potentially advancing the development of new and more effective treatments for this devastating neurodegenerative disease.

Conflict of interests

The authors declare no conflict of interest.

Funding: This project was supported by Coordenação de Aperfeiçoamento de Pessoal de Nível Superior (CAPES, Brazil) through Programa de Excelência Acadêmica (PROEX), Conselho Nacional de Pesquisa e Desenvolvimento Tecnológico (CNPq, Brazil), and Associação para Promoção da Excelência do Software Brasileiro (Softex, Brazil).

References

Adasme, M. F., Linnemann, K. L., Bolz, S. N., Kaiser, F., Salentin, S., Haupt, V. J., & Schroeder, M. (2021). PLIP 2021: Expanding the scope of the protein-ligand interaction profiler to DNA and RNA. *Nucleic Acids Research*, *49*(W1), W530-W534. https://doi.org/10.1093/nar/gkab294. PMid:33950214.

Alabdulraheem, Z. T. J., & Durdagi, S. (2023). Ab initio and comparative 3D modeling of FAM222A-encoded protein and target-driven-based virtual screening for the identification of novel therapeutics against Alzheimer's disease. *Journal of Molecular Graphics & Modelling*, *125*, 108575. https://doi.org/10.1016/j.jmgm.2023.108575. PMid:37552909.

Baell, J. B., & Holloway, G. A. (2010). New substructure filters for removal of pan assay interference compounds (PAINS) from screening libraries and for their exclusion in bioassays. *Journal of Medicinal Chemistry*, *53*(7), 2719-2740. https://doi.org/10.1021/jm901137j. PMid:20131845.

Beaman, E. E., Bonde, A. N., Larsen, S. M. U., Ozenne, B., Lohela, T. J., Nedergaard, M., Gíslason, G. H., Knudsen, G. M., & Holst, S. C. (2023). Blood-brain barrier permeable β-blockers linked to lower risk of Alzheimer's disease in hypertension. *Brain*, *146*(3), 1141-1151. https://doi.org/10.1093/brain/awac076. PMid:35196379.

Breijyeh, Z., & Karaman, R. (2020). Comprehensive review on Alzheimer's disease: Causes and treatment. *Molecules*, *25*(24), 5789. https://doi.org/10.3390/molecules25245789. PMid:33302541.

Das, B., & Yan, R. (2017). Role of BACE1 in Alzheimer's synaptic function. *Translational Neurodegeneration*, *6*(1), 23. https://doi.org/10.1186/s40035-017-0093-5. PMid:28855981.

Davies, S. J., Burhan, A. M., Kim, D., Gerretsen, P., Graff-Guerrero, A., Woo, V. L., Kumar, S., Colman, S., Pollock, B. G., Mulsant, B. H., & Rajji, T. K. (2018). Sequential drug treatment algorithm for agitation and aggression in Alzheimer's and mixed dementia. *Journal of Psychopharmacology*, *32*(5), 509-523. https://doi.org/10.1177/0269881117744996. PMid:29338602.

DeTure, M. A., & Dickson, D. W. (2019). The neuropathological diagnosis of Alzheimer's disease. *Molecular Neurodegeneration*, *14*(1), 32. https://doi.org/10.1186/s13024-019-0333-5. PMid:31375134.

Dolciami, D., Ziolek, R. M., Davies, D. W., Carter, M., Mok, N. Y., & Sherhod, R. (2024). Exploiting vector pattern diversity of molecular scaffolds for cheminformatics tasks in drug discovery. *Journal of Chemical Information and Modeling*, *64*(6), 1966-1974. https://doi.org/10.1021/acs.jcim.3c01674. PMid:38437714.

DrugBank. (2023). *Betaxolol*. https://go.drugbank.com/drugs/DB00195

Enamine. (2023). *Enamine REAL compounds*. https://enamine.net/compound-collections/real-compounds/

Fiscon, G., Sibilio, P., Funari, A., Conte, F., & Paci, P. (2022). Identification of potential repurposable drugs in alzheimer's disease exploiting a bioinformatics analysis. *Journal of Personalized Medicine*, *12*(10), 1731. https://doi.org/10.3390/jpm12101731. PMid:36294870.

FLAML. (2023). https://microsoft.github.io/FLAML/

GitHub. (2023). *Samoturk/mol2vec*. https://github.com/samoturk/mol2vec

Grayson, J. D., Baumgartner, M. P., Santos Souza, C. D., Dawes, S. J., El Idrissi, I. G., Louth, J. C., Stimpson, S., Mead, E., Dunbar, C., Wolak, J., Sharman, G., Evans, D., Zhuravleva, A., Roldan, M. S., Colabufo, N. A., Ning, K., Garwood, C., Thomas, J. A., Partridge, B. M., de la Vega de Leon, A., Gillet, V. J., Rauter, A. P., & Chen, B. (2021). Amyloid binding and beyond: A new approach for Alzheimer's disease drug discovery targeting Aßo–PrPC binding and downstream pathways. *Chemical Science*, *12*(10), 3768-3785. https://doi.org/10.1039/D0SC04769D. PMid:34163650.

Guidotti, I. L., Neis, A., Martinez, D. P., Seixas, F. K., Machado, K., & Kremer, F. S. (2023). Bambu and its applications in the discovery of active molecules against melanoma. *Journal of Molecular Graphics & Modelling*, *124*, 108564. https://doi.org/10.1016/j.jmgm.2023.108564. PMid:37453311.

Hampel, H., Vassar, R., De Strooper, B., Hardy, J., Willem, M., Singh, N., Zhou, J., Yan, R., Vanmechelen, E., De Vos, A., Nisticò, R., Corbo, M., Imbimbo, B. P., Streffer, J., Voytyuk, I., Timmers, M., Tahami Monfared, A. A., Irizarry, M., Albala, B., Koyama, A., Watanabe, N., Kimura, T., Yarenis, L., Lista, S., Kramer, L., & Vergallo, A. (2021). The β-Secretase BACE1 in Alzheimer's disease. *Biological Psychiatry*, *89*(8), 745-756. https://doi.org/10.1016/j.biopsych.2020.02.001. PMid:32223911.

Hassan, M., Shahzadi, S., Yasir, M., Chun, W., & Kloczkowski, A. (2023). Computational prognostic evaluation of Alzheimer's drugs from FDA-approved database through structural conformational dynamics and drug repositioning approaches. *Scientific Reports*, *13*(1), 18022. https://doi.org/10.1038/s41598-023-45347-1. PMid:37865690.

Higaki, J., Murphy Junior, G. M., & Cordell, B. (1997). Inhibition of beta-amyloid formation by haloperidol: A possible mechanism for reduced frequency of Alzheimer's disease pathology in schizophrenia. *Journal of Neurochemistry*, *68*(1), 333-336. https://doi.org/10.1046/j.1471-4159.1997.68010333.x. PMid:8978743.

Huang, W. J., Zhang, X., & Chen, W. W. (2016). Role of oxidative stress in Alzheimer's disease. *Biomedical Reports*, *4*(5), 519-522. https://doi.org/10.3892/br.2016.630. PMid:27123241.

Ivanova, L., & Karelson, M. (2022). The Impact of software used and the type of target protein on molecular docking accuracy. *Molecules*, 27(24), 9041. https://doi.org/10.3390/molecules27249041. PMid:36558174.

Ju Hwang, C., Choi, D.-Y., Park, M. H., & Hong, J. T. (2019). NF-κB as a key mediator of brain inflammation in Alzheimer's disease. *CNS & Neurological Disorders Drug Targets*, *18*(1), 3-10. https://doi.org/10.2174/1871527316666170807130011. PMid:28782486.

Katz, I., de Deyn, P.-P., Mintzer, J., Greenspan, A., Zhu, Y., & Brodaty, H. (2007). The efficacy and safety of risperidone in the treatment of psychosis of Alzheimer's disease and mixed dementia: A meta-analysis of 4 placebo-controlled clinical trials. *International Journal of Geriatric Psychiatry*, *22*(5), 475-484. https://doi.org/10.1002/gps.1792. PMid:17471598.

Kim, Y. D., Jeong, E. I., Nah, J., Yoo, S.-M., Lee, W. J., Kim, Y., Moon, S., Hong, S.-H., & Jung, Y.-K. (2017). Pimozide reduces toxic forms of tau in TauC3 mice via 5′ adenosine monophosphate-activated protein kinase-mediated autophagy. *Journal of Neurochemistry*, *142*(5), 734-746. https://doi.org/10.1111/jnc.14109. PMid:28632947.

Kim, Y., Choi, H., Lee, W., Park, H., Kam, T.-I., Hong, S.-H., Nah, J., Jung, S., Shin, B., Lee, H., Choi, T.-Y., Choo, H., Kim, K.-K., Choi, S.-Y., Kayed, R., & Jung, Y.-K. (2016). Caspase-cleaved tau exhibits rapid memory impairment associated with tau oligomers in a transgenic mouse model. *Neurobiology of Disease*, 87, 19-28. https://doi.org/10.1016/j.nbd.2015.12.006. PMid:26704708.

Kumar, N., Kumar, V., Anand, P., Kumar, V., Ranjan Dwivedi, A., & Kumar, V. (2022). Advancements in the development of multi-target directed ligands for the treatment of Alzheimer's disease. *Bioorganic & Medicinal Chemistry*, *61*, 116742. https://doi.org/10.1016/j.bmc.2022.116742. PMid:35398739.

Kumar, S., Chowdhury, S., & Kumar, S. (2017). In silico repurposing of antipsychotic drugs for Alzheimer's disease. *BMC Neuroscience*, *18*(1), 76. https://doi.org/10.1186/s12868-017-0394-8. PMid:29078760.

Li, F., Wang, Z.-M., Wu, J.-J., Wang, J., Xie, S.-S., Lan, J.-S., Xu, W., Kong, L.-Y., & Wang, X.-B. (2016). Synthesis and pharmacological evaluation of donepezil-based agents as new cholinesterase/monoamine oxidase inhibitors for the potential application against Alzheimer's disease. *Journal of Enzyme Inhibition and Medicinal Chemistry*, *31*(Suppl 3), 41-53. https://doi.org/10.1080/14756366.2016.1201814.

Lombardo, S., & Maskos, U. (2015). Role of the nicotinic acetylcholine receptor in Alzheimer's disease pathology and treatment. *Neuropharmacology*, *96*(Pt B), 255-262. https://doi.org/10.1016/j.neuropharm.2014.11.018. PMid:25514383.

Manzoor, S., & Hoda, N. (2020). A comprehensive review of monoamine oxidase inhibitors as Anti-Alzheimer's disease agents: A review. *European Journal of Medicinal Chemistry*, *206*, 112787. https://doi.org/10.1016/j.ejmech.2020.112787. PMid:32942081.

Marucci, G., Buccioni, M., Ben, D. D., Lambertucci, C., Volpini, R., & Amenta, F. (2021). Efficacy of acetylcholinesterase inhibitors in Alzheimer's disease. *Neuropharmacology*, *190*, 108352. https://doi.org/10.1016/j.neuropharm.2020.108352. PMid:33035532.

Mashour, G. A. (2011). Acetylcholine: Working on working memory. *Science Translational Medicine*, *3*(114), 114ec208. https://doi.org/10.1126/scitranslmed.3003583.

Matthews, D. C., Ritter, A., Thomas, R. G., Andrews, R. D., Lukic, A. S., Revta, C., Kinney, J. W., Tousi, B., Leverenz, J. B., Fillit, H., Zhong, K., Feldman, H. H., & Cummings, J. (2021). Rasagiline effects on glucose metabolism, cognition, and tau in Alzheimer's dementia. *Alzheimer's & Dementia: Translational Research & Clinical Interventions*, *7*(1), e12106. https://doi.org/10.1002/trc2.12106. PMid:33614888.

Medeiros, R., Baglietto-Vargas, D., & LaFerla, F. M. (2011). The role of tau in Alzheimer's disease and related disorders. *CNS Neuroscience & Therapeutics*, *17*(5), 514-524. https://doi.org/10.1111/j.1755-5949.2010.00177.x. PMid:20553310.

Miller, M. B., Huang, A. Y., Kim, J., Zhou, Z., Kirkham, S. L., Maury, E. A., Ziegenfuss, J. S., Reed, H. C., Neil, J. E., Rento, L., Ryu, S. C., Ma, C. C., Luquette, L. J., Ames, H. M., Oakley, D. H., Frosch, M. P., Hyman, B. T., Lodato, M. A., Lee, E. A., & Walsh, C. A. (2022). Somatic genomic changes in single Alzheimer's disease neurons. *Nature*, *604*(7907), 714-722. https://doi.org/10.1038/s41586-022-04640-1. PMid:35444284.

Morris, G. M., Huey, R., Lindstrom, W., Sanner, M. F., Belew, R. K., Goodsell, D. S., & Olson, A. J. (2009). AutoDock4 and AutoDockTools4: Automated docking with selective receptor flexibility. *Journal of Computational Chemistry*, *30*(16), 2785-2791. https://doi.org/10.1002/jcc.21256. PMid:19399780.

Muralidar, S., Ambi, S. V., Sekaran, S., Thirumalai, D., & Palaniappan, B. (2020). Role of tau protein in Alzheimer's disease: The prime pathological player. *International Journal of Biological Macromolecules*, *163*, 1599-1617. https://doi.org/10.1016/j.ijbiomac.2020.07.327. PMid:32784025.

Negrón, A. E., & Reichman, W. E. (2000). Risperidone in the treatment of patients with Alzheimer's disease with negative symptoms. *International Psychogeriatrics*, *12*(4), 527-536. https://doi.org/10.1017/S1041610200006633. PMid:11263718.

O'Reilly, L. P., Knoerdel, R. R., Silverman, G. A., & Pak, S. C. (2016). High-throughput, liquid-based genome-wide RNAi screening in *C. elegans*. *Methods in Molecular Biology*, *1470*, 151-162. https://doi.org/10.1007/978-1-4939-6337-9_12. PMid:27581291.

Podsiedlik, M., Markowicz-Piasecka, M., & Sikora, J. (2022). The influence of selected antipsychotic drugs on biochemical aspects of Alzheimer's disease. *International Journal of Molecular Sciences*, *23*(9), 4621. https://doi.org/10.3390/ijms23094621. PMid:35563011.

Pytel, E., Bukowska, B., Koter-Michalak, M., Olszewska-Banaszczyk, M., Gorzelak-Pabiś, P., & Broncel, M. (2017). Effect of intensive lipid-lowering therapies on cholinesterase activity in patients with coronary artery disease. *Pharmacological Reports*, *69*(1), 150-155. https://doi.org/10.1016/j.pharep.2016.09.016. PMid:27923158.

Raulin, A.-C., Doss, S. V., Trottier, Z. A., Ikezu, T. C., Bu, G., & Liu, C.-C. (2022). ApoE in Alzheimer's disease: Pathophysiology and therapeutic strategies. *Molecular Neurodegeneration*, *17*(1), 72. https://doi.org/10.1186/s13024-022-00574-4. PMid:36348357.

Salentin, S., Schreiber, S., Haupt, V. J., Adasme, M. F., & Schroeder, M. (2015). PLIP: Fully automated protein-ligand interaction profiler. *Nucleic Acids Research*, *43*(W1), W443-7. https://doi.org/10.1093/nar/gkv315. PMid:25873628.

Scheltens, P., Blennow, K., Breteler, M. M. B., de Strooper, B., Frisoni, G. B., Salloway, S., & Van der Flier, W. M. (2016). Alzheimer's disease. *Lancet*, *388*(10043), 505-517. https://doi.org/10.1016/S0140-6736(15)01124-1. PMid:26921134.

Shigeta, M., & Homma, A. (2001). Donepezil for Alzheimer's disease: Pharmacodynamic, pharmacokinetic, and clinical profiles. *CNS Drug Reviews*, *7*(4), 353-368. https://doi.org/10.1111/j.1527-3458.2001.tb00204.x. PMid:11830754.

Sutherland, J. J., Yonchev, D., Fekete, A., & Urban, L. (2023). A preclinical secondary pharmacology resource illuminates target-adverse drug reaction associations of marketed drugs. *Nature Communications*, *14*(1), 4323. https://doi.org/10.1038/s41467-023-40064-9. PMid:37468498.

Swanson, C. J., Zhang, Y., Dhadda, S., Wang, J., Kaplow, J., Lai, R. Y. K., Lannfelt, L., Bradley, H., Rabe, M., Koyama, A., Reyderman, L., Berry, D. A., Berry, S., Gordon, R., Kramer, L. D., & Cummings, J. L. (2021). A randomized, double-blind, phase 2b proof-of-concept clinical trial in early Alzheimer's disease with lecanemab, an anti-Aß protofibril antibody. *Alzheimer's Research & Therapy*, *13*(1), 80. https://doi.org/10.1186/s13195-021-00813-8. PMid:33865446.

Tang, B.-C., Wang, Y.-T., & Ren, J. (2023). Basic information about memantine and its treatment of Alzheimer's disease and other clinical applications. *Ibrain*, *9*(3), 340-348. https://doi.org/10.1002/ibra.12098. PMid:37786758.

Thomé, G. R., Spanevello, R. M., Mazzanti, A., Fiorenza, A. M., Duarte, M. M. M. F., da Luz, S. C. A., Pereira, M. E., Morsch, V. M., Schetinger, M. R. C., & Mazzanti, C. M. (2011). Vitamin E decreased the activity of acetylcholinesterase and level of lipid peroxidation in brain of rats exposed to aged and diluted sidestream smoke. *Nicotine & Tobacco Research: Official Journal of the Society for Research on Nicotine and Tobacco*, *13*(12), 1210-1219. https://doi.org/10.1093/ntr/ntr154. PMid:21896885.

Trott, O., & Olson, A. J. (2010). AutoDock Vina: Improving the speed and accuracy of docking with a new scoring function, efficient optimization, and multithreading. *Journal of Computational Chemistry*, *31*(2), 455-461. https://doi.org/10.1002/jcc.21334. PMid:19499576.

Xiong, G., Wu, Z., Yi, J., Fu, L., Yang, Z., Hsieh, C., Yin, M., Zeng, X., Wu, C., Lu, A., Chen, X., Hou, T., & Cao, D. (2021). ADMETlab 2.0: An integrated online platform for accurate and comprehensive predictions of ADMET properties. *Nucleic Acids Research*, *49*(W1), W5-W14. https://doi.org/10.1093/nar/gkab255. PMid:33893803.

Zeng, X., Zhu, S., Liu, X., Zhou, Y., Nussinov, R., & Cheng, F. (2019). deepDR: A network-based deep learning approach to in silico drug repositioning. *Bioinformatics*, *35*(24), 5191-5198. https://doi.org/10.1093/bioinformatics/btz418. PMid:31116390.

Zhang, L., Yu, J., Pan, H., Hu, P., Hao, Y., Cai, W., Zhu, H., Yu, A. D., Xie, X., Ma, D., & Yuan, J. (2007). Small molecule regulators of autophagy identified by an image-based high-throughput screen. *Proceedings of the National Academy of Sciences of the United States of America*, *104*(48), 19023-19028. https://doi.org/10.1073/pnas.0709695104. PMid:18024584.

Zhang, X.-X., Tian, Y., Wang, Z.-T., Ma, Y.-H., Tan, L., & Yu, J.-T. (2021). The epidemiology of Alzheimer's disease modifiable risk factors and prevention. *The Journal of Prevention of Alzheimer's Disease*, *8*(3), 313-321. https://doi.org/10.14283/jpad.2021.15. PMid:34101789.

Zhu, T., Cao, S., Su, P.-C., Patel, R., Shah, D., Chokshi, H. B., Szukala, R., Johnson, M. E., & Hevener, K. E. (2013). Hit identification and optimization in virtual screening: Practical recommendations based upon a critical literature analysis. *Journal of Medicinal Chemistry*, *56*(17), 6560-6572. https://doi.org/10.1021/jm301916b. PMid:23688234.

ZINC. (2023). https://zinc.docking.org/

Supplementary Material

Supplementary material accompanies this paper.

Supplementary Data 1. Potential protein targets of Alzheimer's Disease and their respective 3D structures available at PDB, including amino acid residues relevant for docking analysis (potentially related to activity) derived from literature.

Supplementary Data 2. Classification (y-randomization and test) metrics computed for the QSAR models for all evaluated estimators produced by Bambu based on different High-Throughput Screening (HTS) studies obtained from PubChem BioAssays. The best model for each HTS study was selected based on the F1-score.

Supplementary Data 3. Chemical space analysis of the HTS datasets and the FDA dataset based on 2048 Morgan Fingerprints and 2D UMAP embeddings. The Convex Hull was generated using the SciPy library.

Supplementary Data 4. Ranked list of molecules identified as potential candidates for Alzheimer's Disease multi-target drugs by a collection of Bambu QSAR models from a dataset of FDA-approved medications.

Supplementary Data 5. Ranked list of refined molecules identified as potential candidates for Alzheimer's Disease multi-target drugs using molecular docking analysis.

This material is available as part of the online article from https://doi.org/10.4322/biori.00072025